



Photonic based Radar: Characterization of 1x4 Mach- Zehnder Demultiplexer

Umar Shahzad

Supervised by: Dr. Antonella Bogoni

Master in Computer Science and Networking

Acknowledgement

First and foremost, my utmost gratitude and deep appreciation goes to my supervisor, Prof. Antonella Bogoni; and Filippo Scotti for their kindness, constant endeavour, guidance and the numerous moments of attention they devoted throughout this work. I would like to thank my supervisor for proposing the idea for this work and introducing me to the world of Digital Photonics.

I would also like to thank Scuola Superiore Sant'anna TeCIP for providing me a complete friendly research environment to accomplish this work.

Special thanks go to my family members for their unconditional support on this endeavour of mine. At the end, I would like to acknowledge the financial, academic and technical support of the University of Pisa and want to thank the Master Board for providing me such opportunity.

Abstract

This work is based on a research activity which aims to implement an optical transceiver for a photonic-assisted fully-digital radar system based on optical miniaturized optical devices both for the optical generation of the radiofrequency (RF) signal and for the optical sampling of the received RF signal. The work is more focused on one very critical block of receiver which is used to parallelize optical samples. Parallelization will result in samples which will be lower in repetition rate so that we can use commercial available ADCs for further processing. This block needs a custom design to meet all the system specifications. In order to parallelize the samples a 1x4 switching matrix (demux) based on Mach Zehnder (MZ) interferometer has been proposed. The demux technique is Optical Time Division Demultiplexing. In order to operate this demux according to the requirements the characterization of device is needed. We need to find different stable control points (coupler bias and MZ bias) of demux to get output samples with high extinction ratio. A series of experiments have been performed to evaluate the matrix performance, issues and sensitivity. The evaluated results along with the whole scheme have been discussed in this document.

Contents

1. INTRODUCTION	1
1.1. Introduction to Thesis	1
1.2. All Optical Signal Processing	3
1.2.1. Why Optical Processing over Electronics with some background	3
1.2.2. Some Developments	7
1.2.3. Limitations	12
1.3. Basics of Radar Principle	13
1.3.1. A Short History	14
1.3.2. Radar Basic Operational Principle	16
2. Radar Systems	20
2.1. Classification of Radar Systems	20
2.1.1. Depending on Technologies	20
2.1.1.1. Continuous Wave (CW) Radar	22
2.1.1.2. Frequency Modulated CW (FMCW) Radar	25
2.1.1.3. Bistatic Radar Set	29
2.1.1.4. Moving Target Indication (MTI) Radar	30
2.1.1.5. Pulse Doppler Radar	34
2.1.1.6. Pulse Compression in Radar	34
2.1.2. Depending on Design	36
2.1.2.1. Air-Defence Radars	36
2.1.2.2. Air Traffic Control (ATC)-Radars	37
2.2. Coherent and Non-Coherent Processing in Radars	39

2.3. Radar Devices	40
2.3.1. Transmitter	40
2.3.1.1. Pseudo-coherent or Non-coherent Radar	41
2.3.1.2. Coherent Radar	45
2.3.2. Radar receiver	48
2.3.2.1. Super-heterodyne Receiver	48
2.4. Some limitations	51
3. Photonic based Radar: Characterization of 1x4 Mach-Zehnder Demux	52
3.1. Overall Scenario	52
3.1.1. Radio Frequency (RF) generation	52
3.1.2. Radar Receiver	56
3.1.2.1. Photonic Sampled and electronically Quantized ADCs	59
3.2. Characterization of 1x4 Mach-Zehnder Demultiplexer (demux)	62
3.2.1. Technological aspects	63
3.2.2. Mach Zehnder as Switch	65
3.2.3. Matching and Biasing network	66
3.2.4. Coupler Bias Voltage ($V_{\text{bias coup}}$)	68
3.2.5. Critical Observations	75
4. Conclusion	77
4.1. Current Status of Experiments	77
4.1.1. Driving Signal amplification and tuning	78
4.1.2. Experiment Results	80
5. References	82

1. Introduction

1.1. Introduction to Thesis

In modern radar system in order to meet the requirements of high resolution, sensitivity and flexibility the limitations in current electronic systems have to be overcome. Coherent radar systems detect moving objects with excellent discrimination from weather and background clutter, by extracting information from the phase of the echoes [1]. In order to meet the required performance, the phase noise of the radar signal must be reduced as much as possible. The spectral purity of the RF signals generated by electronic architectures is mainly limited by the noisy frequency multiplication that worsens the signal quality as the required frequency increases. The first requirement is to generate an RF signal which should be phase coherent and able to achieve very high frequencies. The technologies which can provide a significant benefits in terms of phase coherence, fast processing and high frequency generation can rule the future radar world.

The second requirement is the efficient processing of the received signal along with the deduction of those conventional electronic processes that lead to noise and distortion. The conventional electronic radar receiver architecture also adds phase noise by frequency multiplication, down-conversion; to shift the original frequency to an intermediate value where the electrical analog-to-digital converters (ADCs) can be exploited. This element is the main reason of distortions and phase noise. As far as ADCs are concerned, the ability to implement flexible and high resolution digital-receiver architectures is often limited by the performance of the ADC component. For example, electronic ADCs with sampling rates > 1 GS/s (giga-sample per second) are presently limited to resolutions of less than 7 effective bits

[44-dB signal-to-noise ratio (SNR)] [2] and ADCs having 12 effective bits (74-dB SNR) have a maximum sampling rate of 65 MS/s (mega-sample per second).

In order to overcome the problems in current radar systems photonic solution proves to be an alternative. The generation of RF signals in photonics allow the development of a radar transmitter with high phase coherence, and ultra-high microwave frequency. As far as receivers are concerned, radar systems could benefit significantly from high-resolution (12 bits) ADCs having mutli-gigahertz of instantaneous bandwidth. The flexibility of the receivers in these systems can be augmented by pushing the ADC closer to the antenna and performing more of the receiver functions in the digital domain. Photonic solutions for ADC can be used to sample the received RF signal in photonic domain, which result in high sampling rate and high resolution. This way down-conversion process can be avoid.

This thesis work is based on a research activity which aims to implement an optical transceiver for a photonic-assisted fully-digital radar system based on optic miniaturized optical devices both for the optical generation of the radiofrequency (RF) signal and for the optical sampling of the received RF signal. This thesis is focused on one very critical block of receiver which is used to parallelize optical samples. Parallelization will result in samples which will be lower in repetition rate so that we can use commercial available ADCs for further processing. This block needs a custom design to meet all the system specifications. In order to parallelize the samples a 1x4 switching matrix (demux) based on Mach Zehnder (MZ) interferometer has been proposed. The demux technique is Optical Time Division Demultiplexing. Electro-optic technology has been used in the design of the switching matrix to reduce the cost. In order to operate this demux according to our requirement the characterization of device is needed. We need to find different stable control points (coupler bias and MZ bias) of demux to get output samples with high extinction ratio. I have performed a number of experiments in the Lab to evaluate the matrix performance, issues and sensitivity.

Rest of this chapter is focused on the importance of all optical processing, some developments and limitations in this regards and finally basics of radar system.

1.2. All Optical Signal Processing

1.2.1. Why Optical Processing over Electronics Processing with some background

The dielectric waveguide proposed by Kao and Hockham in 1966 for guiding lightwaves have revolutionized the transmission of broadband signals and ultrahigh capacity over ultra-long global telecommunication systems and networks. In the 1970s, the reduction of the fiber losses over the visible and infrared spectral regions was extensively investigated. Since then, the research, development, and commercialization of optical fiber communication systems progressed with practical demonstrations of higher and higher bit rates and longer and longer transmission distance. Significantly, the installation of optical fiber systems was completed in 1978. Since then, fiber systems have been installed throughout the world and interconnecting all continents of the globe with terrestrial and undersea systems.

The primary reason for such exciting research and development is that the frequency of the lightwave is in the order of a few hundred terahertz and the low loss windows of glass fiber are sufficiently wide so that several tens of terabits per second capacity of information can be achieved over ultra-long distance, whereas the carrier frequencies of the microwave and millimeter-wave are in the tens of gigahertz [3]. Indeed in the 1980s, the transmission speed and distance were limited because of the ability of regeneration of information signals in the optical or photonic domain. Data signals were received and recovered in the electronic domain; then the lightwave sources for retransmission were modulated. The distance between these regenerators was limited to 40 km for installed fiber transmission systems. Furthermore, the dispersion-limited distance was longer than that of the attenuation-limited distance, and no compensation of dispersion was required.

The distance without repeater could then be extended to another 20 km with the use of coherent detection techniques in the mid-1980s; heterodyne and homodyne techniques were extensively investigated. But applications of coherent processing restrict due to phase estimation (local oscillator for mixing) at receiver and complexity [3]. The attenuation was eventually overcome with the invention of the optical amplifiers in 1987 using Nd or Er doping in silica fiber. Optical gain of 20–30 dB can be easily obtained. Hence, the only major issue was the dispersion of lightwave signals in long-haul transmission. This leads to extensive search for the compensation of dispersion. The simplest method can be the use of

dispersion compensating fibers inserted in each transmission span, hence the phase reversal of the lightwave and compensation in the photonic domain. This is a form of photonic signal processing [3].

This leads to the development of high and ultrahigh bit rate transmission system. The bit rate has reached 10, 40, and 80 Gb/s per wavelength channels in the late 1990s. Presently, the transmission systems of several wavelength channels each carrying 40 Gb/s are practically proven and installed in a number of routes around the world. With the passage of time the trend is moving forward to attain ultrafast speed but to process these fast signals in electronics is no longer possible due to bandwidth limitation of electronics and thus signal processors in the photonic domain are expected to play a major role in these fast systems.

All optical processing can also be beneficial over electronics in term of power consumption. Energy efficiency is becoming one of the key factors in almost every aspect of daily life. The energy efficiency in the internet has recently been a hot topic due to growth of Internet Traffic, which is keep on growing. Figure 1.1 shows the trend of total IP data traffic growth worldwide, which is an average of 32% annually, between 2010 and 2015, reaching approximately 80 exabytes (80 million terabytes) per month by 2015 [4]. The increasing popularity of mobile terminals, especially smartphones, is further spurring data traffic. By allowing users to access data-rich content through the Internet almost anywhere and anytime, smartphones are generating 10 to 20 times more data traffic than conventional mobile phones [4]. Figure 1.2 shows the trend of business IP traffic growth which is escalating worldwide and “cloud computing” playing a big role in this growth.

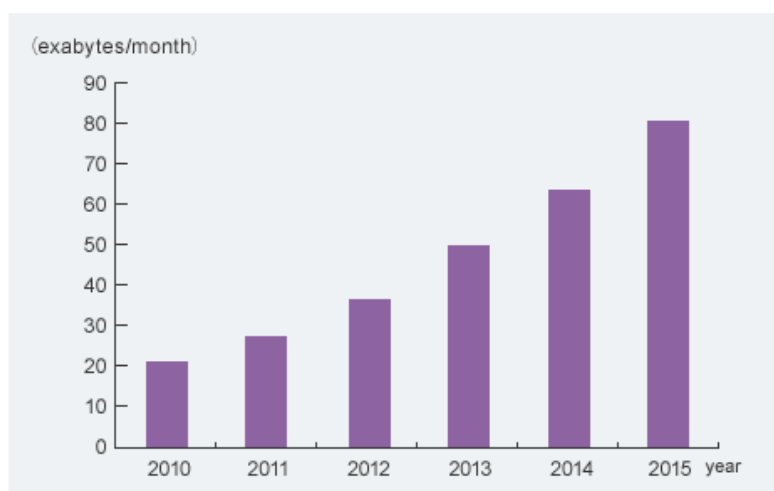


Figure 1.1. Cisco Systems, Inc. estimates that global IP traffic will reach approxi-

mately 80 exabytes per month by 2015.

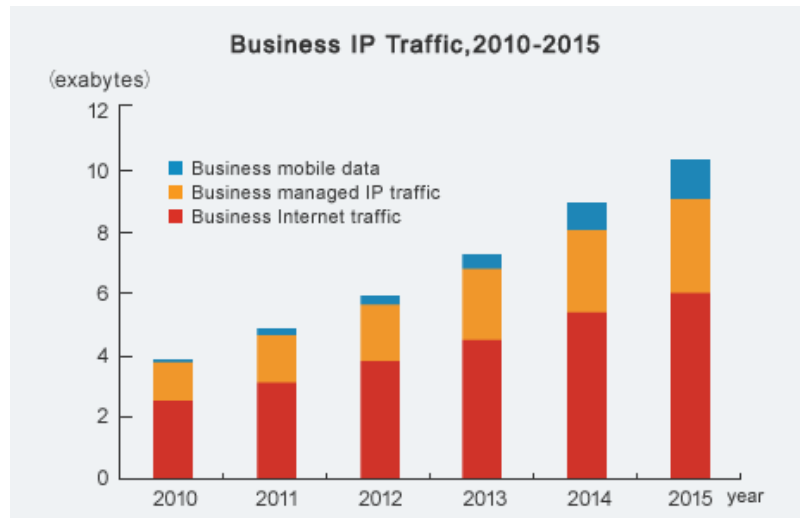


Figure 1.2. Business IP traffic is expected to increase annually by an average of 22% between 2010 and 2015, reaching approximately 10 exabytes (10 million terabytes) per month by 2015

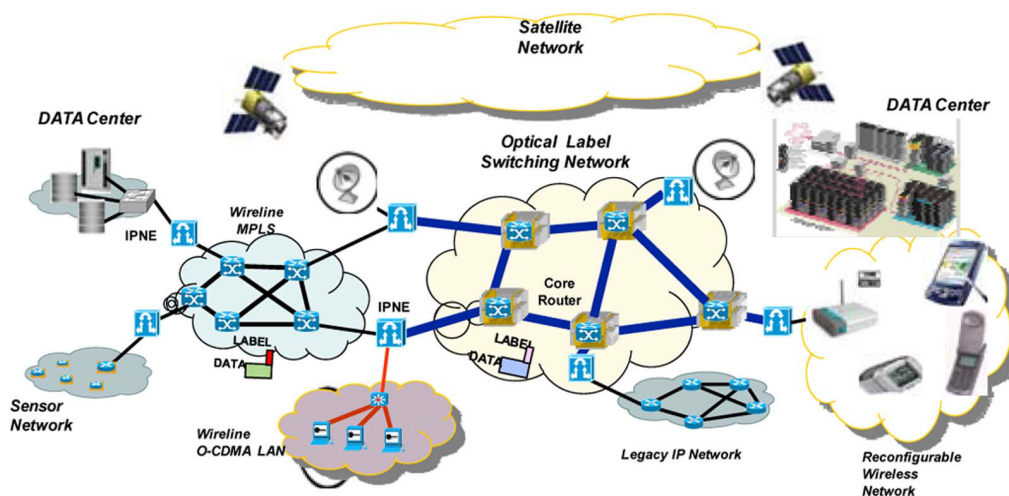
This explosive growth leads to the need of energy efficient high capacity systems. In this scenario, all optical processing can be a big alternative because it has already been proven that high speed and energy efficiency can be achieved from photons. From Figure 1.3 below it can be analysed, by keeping in mind the increasing growth of Internet Traffic, that why is it so important to go towards energy efficiency in ICT.



Figure 1.3. A view of Power Consumption

In order to well establish a point, mentioned in above paragraphs, that all optical processing can be an attractive alternative over electronics let us consider two examples from

current network scenario. The Figure 1.4 below shows the schematic of internet today depicting the complex heterogeneity of internet. The user may run a variety of applications across wireless, wireline, and optical technologies running many different protocols. Packets intended to run same applications between peers may take different paths based on wireless, wireline, and/or optical technologies. In this situation, unified networking platform with high capacity (optical layer) will be a real advantage [5]. If Internet packets process completely in optical domain, while passing through the landline network, then we will attain a high capacity power efficient system. Here it is worth mention that Electro-Optic conversion is also not energy efficient.



.Figure 1.4.Complex Heterogeneity of today Internet

Another scenario is the all-optical short-range photonic interconnection networks. The main hindrance in the improvement of the present high performance computing systems is the bottleneck of the chip-to-chip and chip-to-memory communication. The limits are the high wiring density, the high power consumption and the limited throughput [6]. Photonic interconnection networks can overcome the limitations of the electronic interconnection networks by guaranteeing high bit rate communications, data format transparency and electromagnetic field immunity. Moreover they can reduce the wiring density and the power consumption. In such networks photonic digital processing can be the most suitable paradigm for simple and ultra-fast control and switching operations, since it reduces the packet latency to the optical time-of-flight.

Beside power consumption and high capacity, below mentioned are some other advantages of all optical processing.

- High spectral and spatial coherence.
- RF interference free.
- Robustness to the cosmic radiations.
- Low distortions in signal distribution.

1.2.2. Some Developments

The idea of all optical processing is to process the signals while they are still in the photonic domain. The first proposal of the processing of signals in the optical/photonic domain was coined by Wilner and van der Heuvel in 1976 [7] indicating that the low loss and broadband transmittance of the single-mode optical fibers would be the most favourable condition for processing of broadband signals in the optical/photonic domain. Since then, several topical developments in this field, including integrated optic components, subsystems, and transmission systems have been reported and contributed to optical communications. Almost all traditional functions in electronic signal processing have been realized in the optical/photonic domain.

In order to apply photonic processing (digital) for the controlling of the network data plane, complex functions must be available. Recent developments in photonic digital processing have been very well summarized in [8]. Below a brief description is mentioned.

Logic Gates

Elementary logic gates as AND, NOR, NAND, NOT has been demonstrated with fibre, waveguide and semiconductor-based solutions. A fibre-based scheme exploits Cross Phase Modulation (XPM) in nonlinear optical loop mirrors structures shown in Figure 1.5 a). A combination of pump depletion and Sum Frequency and Difference Frequency Generation (SFG-DFG) has been exploited in a single Periodically Poled Lithium Niobate (PPLN) waveguide in shown in Figure 1.5 b) to obtain multiple basic logic operations. The logical gates based on Semiconductor solutions exploit Semiconductor Optical Amplifiers (SOAs) followed by optical filtering as shown in Figure 1.5 c). Some other variants of SOA based

gates are: integrated SOAs in Mach Zehnder configuration Figure 1.5 d), passive nonlinear etalons exploiting absorption saturation [9] and semiconductor micro-resonators Figure 1.5 e).

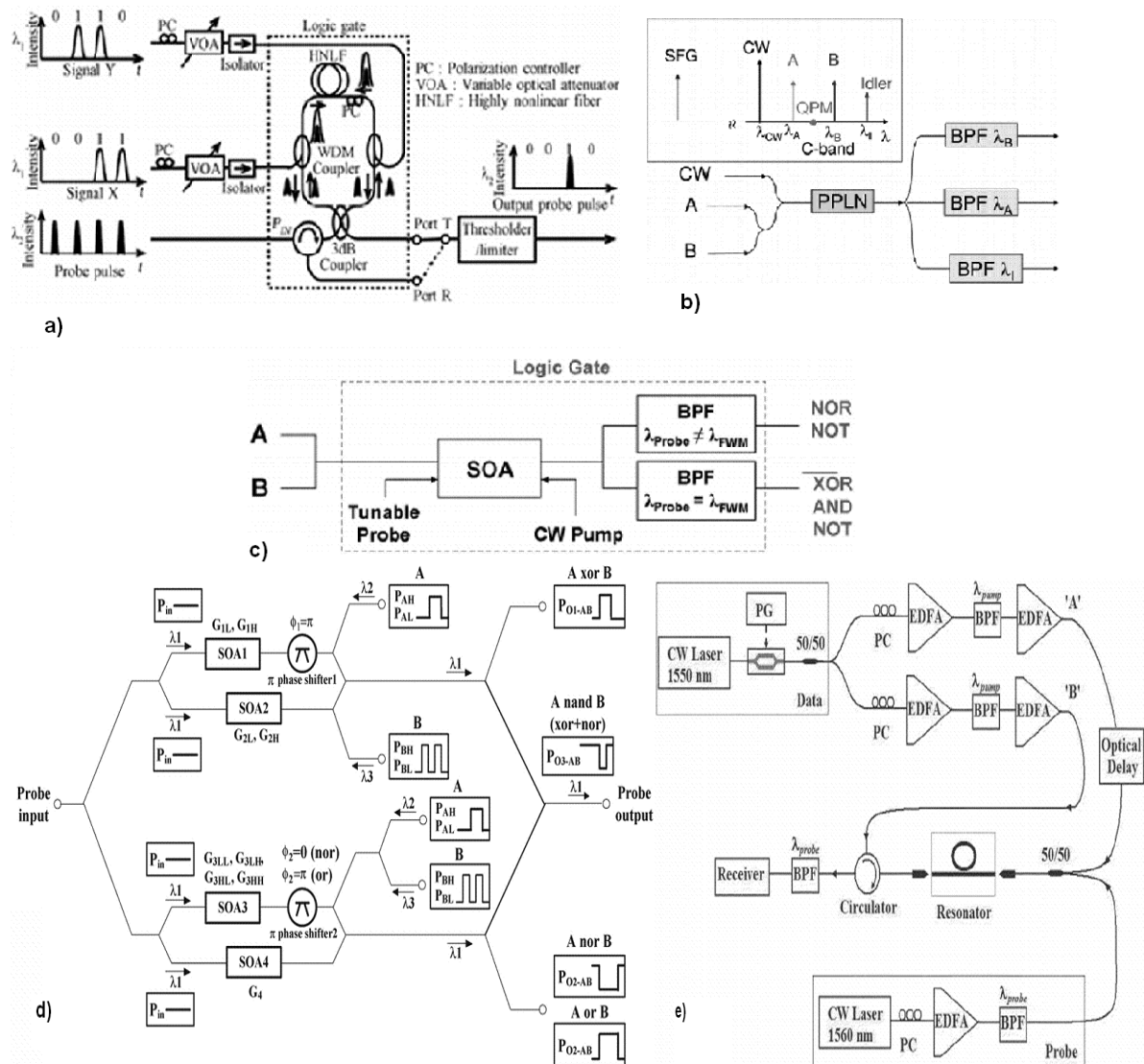


Figure 1.5. Block Diagrams of different techniques to realize Logic Gates

Combinatorial Circuit

An all-optical combinatorial network, for managing the contentions and the switch control in a node of an optical packet switched network, is demonstrated by M. Scaffardi, et al. which is important for the control of all-optical interconnection networks. Figure 1.6 shows the: a) Physical schematic setup, b) Logical circuit and c) Experimental setup of combinatorial network. Similarly other circuits based on Logical gates have been demonstrated which involves:

- All-optical circuits for the pattern matching, i.e. able to determine if two Boolean numbers are equal or not. Pattern matching by a XOR gate implemented with a nonlinear optical loop mirror, by combining AND and XOR gates in a single Semiconductor Optical Amplifier-Mach Zehnder Interferometer (SOA-MZI). The cascade of SOA-MZI structures in order to have a single output pulse in case of matching.
- An SOA-based all-optical circuit for the comparison of 1-bit binary numbers.
- Finally an all optical subsystem able to discriminate if an N-bit (with $N > 1$) pattern representing a binary number is greater or lower than another one is also demonstrated.

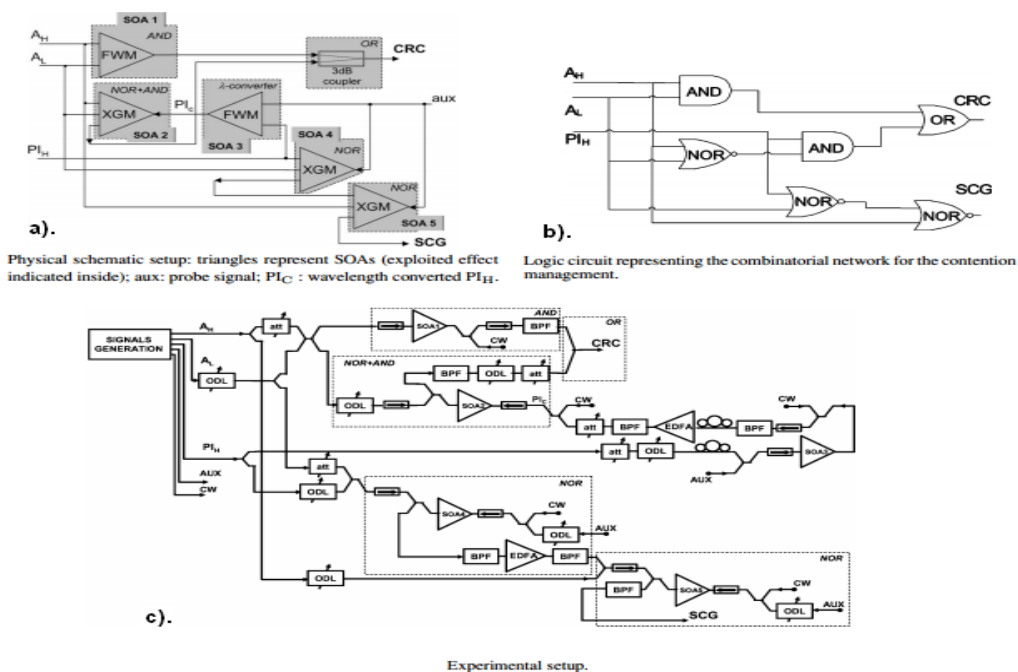


Figure 1.6. Setup of all-optical combinatorial network

Calculating the addition of binary numbers is another important functionality to perform packet header processing. A Time-To-Live (TTL) field represents the maximum number of hops of a packet and it is decremented after each node. When the field value is zero, the packet is discarded and in this way avoids loop formation. So, to implement this functionality an all-optical processing circuit able to perform the decrementing of the binary number in the TTL field requires. Applying the compliments of all optical full-adder, this operation can be performed. Moreover there are also many other applications of full-adder

like resolving the Viterbi algorithm in the Maximum-Likelihood Sequence Estimation (MLSE) etc. An all-optical implementation of full-adder is fast and can improve of circuits. Up to now few works report on the implementation of all-optical full-adders.

- A.J. Poustie, et al. in 1999 employed SOA in a terabit optical asymmetric demultiplexer configuration. The reported operation speed is below 1 Gb/s.
- A faster full-adder based on SOAs is reported by J. H. Kim, et al. in 2003, but in that scheme the output sum depends directly on the input carry; moreover performances in terms of bit error-rate and eye opening are not reported.
- In the SOA-based solution presented by M. Scaffardi, et al. in 2008 the sum and the output carry do not depend directly on the input carry signal, thus potentially improving the output signal quality when cascading multiple full-adders.
- Finally a very fast half-adder and subtractor based on PPLN waveguide is reported in 2009 by A. Bogoni et al.

Flip-flops

Another important subsystem is the flip-flop. It generates a continuous optical signal controlled by pulsed optical signals and allows the control of optical switches. Flip-flops are demonstrated with Erbium-doped fibres Figure 1.7, and with integrated solutions.

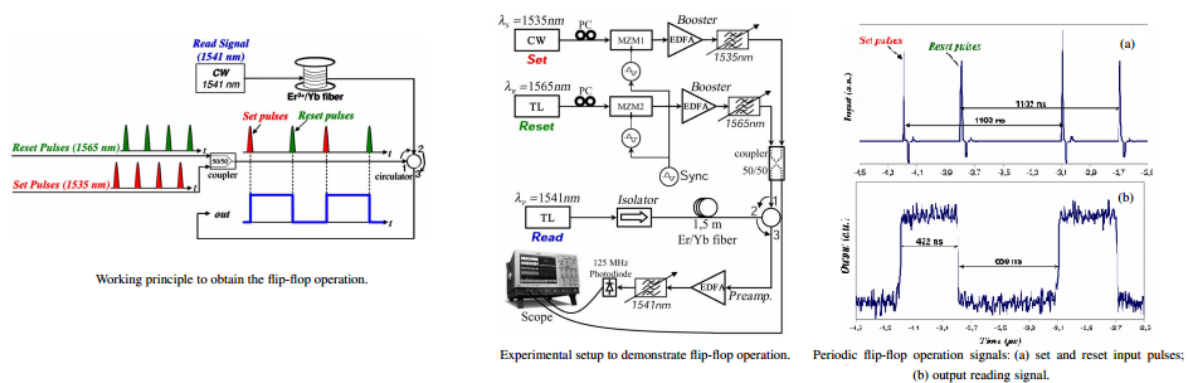


Figure 1.7. Flip-flop based on Erbium-doped fibres

Some other Interesting solutions are based on coupled laser diodes, nonlinear polarization switches, and coupled Mach-Zehnder interferometers. However the solution based on

coupled ring lasers is demonstrated by A. Malacarne, et al. in 2008, presents some advantages as high contrast ratio, symmetric operations for set and reset and large input wavelength range. The slow falling and rising edges of the flip-flop output signal is one of the most critical aspects. Photonic processing on the flip-flop outputs can contribute to reduce the falling and rising edge issues.

Switches and Add/drop modules

Other important basic elements for next generation optical networks are all-optical switches and add/drop modules with Pico-second characteristic times, able to forward optical packet without bit loss or to select single tributary channels from Optical Time Division Multiplexing (OTDM) frames at very high bit rate (100 Gb/s and beyond). Highly nonlinear fiber, nonlinear waveguide or SOA have been used for implementing ultra-fast switching operation. Moreover new very promising silicon-based devices have been developed with advantages in terms of cost, power consumption and CMOS compatibility by C.A. Barrios in 2004.

Photonic ADC and DAC

Photonic digital processing requires Analog-to-Digital and Digital-to-Analog Converters (ADCs and DACs). Electronic A/D conversion is demonstrated up to 40 Gsamples/s with a 3-bit coding by W. Cheng, et al. in 2004. Nevertheless electronic A/D conversion is mainly limited by the ambiguity of the comparators and jitter of the sampling window [10]. The use of hybrid techniques employing an optical signal as sampling signal improves the performances. In 2007 Wangzhe Li, et al. used polarization differential interference and phase modulation to realize all-optical ADC, Figure 1.8 shows the schematic and experimental setup of the technique. Optical sampling with amplitude modulators and time and wavelength-interleaved pulses is demonstrated in [11]. In the last two mentioned techniques the quantization and coding are exploited in the electronic domain. Likewise different hybrid and all-optical techniques for ADC have been demonstrated over the time by utilizing photonic processing i.e. Kerr-effect, nonlinear optical loop mirror (NOLM), self-phase modulation (SPM), and cross gain modulation (XGM) in SOAs etc. SOAs based approach enables analog-to-digital conversion with low optical power requirements with respect to the fiber-based implementations and allows integrated solutions. Optical DAC is

appealing for its possible application in pattern recognition, and arbitrary waveform generation for radar and display applications. S. Oda, and A. Maruta in 2006 and C. Porzi, et al. in 2009 presented some of the DAC approaches.

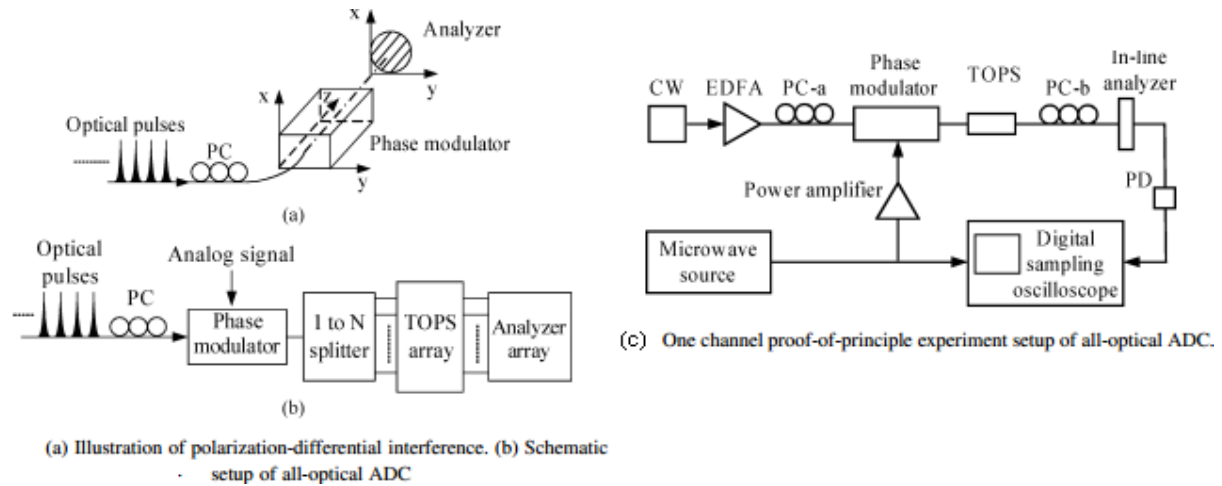


Figure 1.8. All-Optical ADC based on polarization differential interference and phase modulation

In conclusion, the possibility of using single basic building gates for implementing all more complex logic functions seems to be the most practical approach. Nevertheless the photonic digital processing is effective and attractive if it can be realised with integrated solutions. SOAs have shown to be attractive because of their compactness, stability, low switching energy and low latency. Therefore SOA based hybrid integrated solutions represent a first step towards the integration of such complex functionalities. On the other hand the development of silicon photonics makes photonic processing more attractive for green and low cost solutions and it represents a turning point in the next generation optical network evolution. Of course technology development and cross-fertilization between technology and system fields are key issues to make photonic digital processing the basis of the future networks.

1.2.3. Limitations

Photonic processing is in its early stage and the realisation of complete all-optical computing system is still far, no all kind of digital photonic processors have been implemented till now. Already proposed prototype performances are still not comparable with electrical digital processors. Photonic technologies are not mature enough to take the

place of electronics, which is well matured. Technologies issues are at the moment the main limitation to the photonic digital processing development. Lacking of efficient all-optical memories is a big hurdle in all-optical systems currently. Electrons have an advantage over photons that they can store information. Some proposal has been presented to realize buffer functionality but again far from implementation phase. Integration is another issue currently in all-optical processing although some prototype has been proposed. If experimental setups of above mentioned developments have been followed then one can easily put integration under limitation of all-optical processing. Emerging novel optical technologies, such as nanostructured photonic crystal devices, high-contrast silicon optics, or semiconductor quantum dots, promise to decrease the size and power dissipation of photonic integrated circuits to the point where highly integrated systems on a chip can be envisioned. These technologies are far from being mature, and much research has still to be done.

1.3. Basics of Radar Principle

Radar (**R**adio **D**etection **A**nd **R**anging) is an electromagnetic system for object-detection and to determine the range, altitude, direction, or speed of objects. It can be used to detect aircraft, ships, spacecraft, guided missiles, motor vehicles, weather formations, and terrain. The radar dish or antenna transmits pulses of radio waves or microwaves, a pulse-modulated sine wave for example, which bounce off any object in their path. The object returns a tiny part of the wave's energy to a dish or antenna which is usually located at the same site as the transmitter. Radar is used to extend the capability of one's senses for observing the environment, especially the sense of vision. Radar can be designed to see through those conditions impervious to normal human vision, such as darkness, haze, fog, rain and snow. In addition, the most important attribute of radar is of being able to measure the distance or range to the object, which is not possible with human vision.

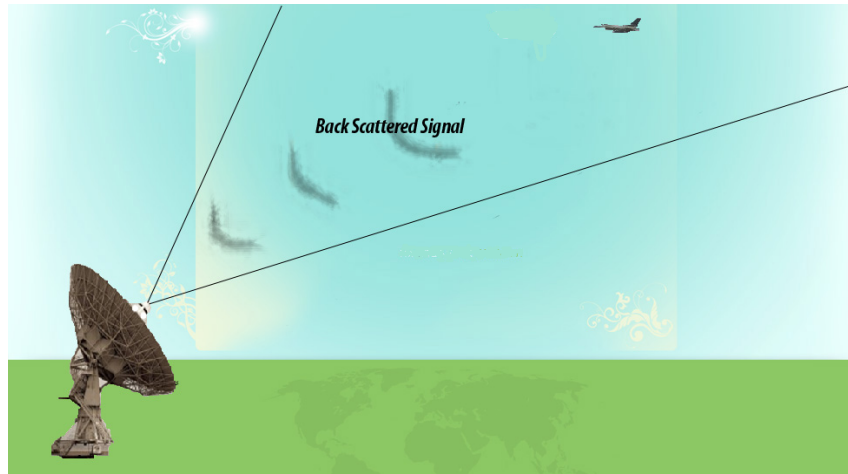


Figure 1.9. Radar basic principal

1.3.1. A Short History

Neither a single nation nor a single person can say that the discovery and development of radar technology was his (or its) own invention. One must see the knowledge about “Radar” than an accumulation of many developments and improvements, in which any scientists from several nations took part in parallel.

As early as 1865, The Scottish physicist **James Clerk Maxwell** presents his *Theory of the Electromagnetic Field* (description of the electromagnetic waves and their propagation) He demonstrated that electric and magnetic fields travel through space in the form of waves, and at the constant speed of light. In 1886, **Heinrich Hertz** showed that radio waves could be reflected from solid objects. In 1895 **Alexander Popov**, a physics instructor at the Imperial Russian Navy school in Kronstadt, developed an apparatus using a coherer tube for detecting distant lightning strikes. The next year, he added a spark-gap transmitter. In 1897, while testing this in communicating between two ships in the Baltic Sea, he took note of an interference beat caused by the passage of a third vessel. In his report, Popov wrote that this phenomenon might be used for detecting objects, but he did nothing more with this observation.

The **German Christian Huelsmeyer** was the first to use radio waves to detect "the presence of distant metallic objects". In 1904 he demonstrated the feasibility of detecting a ship in dense fog but not its distance. He obtained a patent for his detection device in April 1904 and later a patent for a related amendment for determining the distance to the ship. He

also got a British patent on September 23, 1904 for the first full radar application, which he called *telemobiloscope*. In August 1917 **Nikola Tesla** outlined a concept for primitive radar units. He stated, "...by their (standing electromagnetic waves) use we may produce at will, from a sending station, an electrical effect in any particular region of the globe; (with which) we may determine the relative position or course of a moving object, such as a vessel at sea, the distance traversed by the same, or its speed."

In 1922 **A. Hoyt Taylor** and **Leo C. Young**, researchers working with the U.S. Navy, discovered that when radio waves were broadcast at 60 MHz it was possible to determine the range and bearing of nearby ships in the Potomac River. Despite Taylor's suggestion that this method could be used in low visibility, serious investigation began eight years later after the discovery that radar could be used to track airplanes.

Before the Second World War, researchers in France, Germany, Italy, Japan, the Netherlands, the Soviet Union, the United Kingdom, and the United States, independently and in great secrecy, developed technologies that led to the modern version of radar. Australia, Canada, New Zealand, and South Africa followed pre-war Great Britain, and Hungary had similar developments during the war.

In 1934 the **Frenchman Émile Girardeau** stated he was building an obstacle-locating radio apparatus "conceived according to the principles stated by Tesla" and obtained a patent for a working system, a part of which was installed on the Normandie liner in 1935. During the same year, the Soviet military engineer **P.K.Oschepkov**, in collaboration with Leningrad Electro-physical Institute, produced an experimental apparatus, RAPID, capable of detecting an aircraft within 3 km of a receiver. The French and Soviet systems, however, had continuous-wave operation and could not give the full performance that was ultimately at the centre of modern radar.

Full radar evolved as a pulsed system, and the first such elementary apparatus was demonstrated in December 1934 by **American Robert M. Page**, working at the Naval Research Laboratory. The following year, the United States Army successfully tested primitive surface to surface radar to aim coastal battery search lights at night. This was followed by a pulsed system demonstrated in May 1935 by **Rudolf Kühnhold** and the firm GEMA in Germany and then one in June 1935 by an Air Ministry team led by **Robert**

A. Watson Watt in Great Britain. Later, in 1943, Page greatly improved radar with the mono-pulse technique that was used for many years in most radar applications.

The British were the first to fully exploit radar as a defence against aircraft attack. This was spurred on by fears that the Germans were developing death rays. The Air Ministry asked British scientists in 1934 to investigate the possibility of propagating electromagnetic energy and the likely effect. Following a study, they concluded that a death ray was impractical but that detection of aircraft appeared feasible. **Robert Watson Watt's** team demonstrated to his superiors the capabilities of a working prototype and then patented the device. It served as the basis for the Chain Home network of radars to defend Great Britain. In April 1940, *Popular Science* showed an example of a radar unit using the Watson-Watt patent in an article on air defence, but not knowing that the U.S. Army and U.S. Navy were working on radars with the same principle, stated under the illustration, "This is not U.S. Army equipment." Also, in late 1941 *Popular Mechanics* had an article in which a U.S. scientist conjectured what he believed the British early warning system on the English east coast most likely looked like and was very close to what it actually was and how it worked in principle.

The war precipitated research to find better resolution, more portability, and more features for radar, including complementary navigation systems like Oboe used by the RAF's Pathfinder.

1.3.2. Radar Basic Operational Principle

The basic principle of operation [12] of primary radar is simple to understand. However, the theory can be quite complex. Some laws of nature have a greater importance here. Radar measurement of range, or distance, is made possible because of the properties of radiated electromagnetic energy.

1. Reflection of electromagnetic waves: The electromagnetic waves are reflected if they meet an electrically leading surface. If these reflected waves are received again at the place of their origin, then that means an obstacle is in the propagation direction.

2. Electromagnetic energy travels through air at a constant speed, at approximately the speed of light,

- 300,000 kilometres per second or
- 186,000 statute miles per second or
- 162,000 nautical miles per second.

This constant speed allows the determination of the distance between the reflecting objects (airplanes, ships or cars) and the radar site by measuring the running time of the transmitted pulses.

3. This energy normally travels through space in a straight line, and will vary only slightly because of atmospheric and weather conditions. By using special radar antennas this energy can be focused into a desired direction. Thus the direction (in azimuth and elevation) of the reflecting objects can be measured.

These principles can basically be implemented in a radar system, and allow the determination of the distance, the direction and the height of the reflecting object. (There will be the effects of atmosphere and weather on the transmitted energy; however, for this discussion on determining range and direction, these effects will be temporarily ignored.)

The below combination of figures show the operating principle of a primary radar set. The radar antenna illuminates the target with a microwave signal, which is then reflected and picked up by a receiving device. The electrical signal picked up by the receiving antenna is called echo or return. The radar signal is generated by a powerful transmitter and received by a highly sensitive receiver.

All targets produce a diffuse reflection i.e. it is reflected in a wide number of directions. The reflected signal is also called scattering. Backscatter is the term given to reflections in the opposite direction to the incident rays. Radar signals can be displayed on the traditional plan position indicator (PPI) or other more advanced radar display systems. A PPI has a rotating vector with the radar at the origin, which indicates the pointing direction of the antenna and hence the bearing of targets.

Transmitter: The radar transmitter produces the short duration high-power RF pulses of energy that are into space by the antenna.

Duplexer: The duplexer alternately switches the antenna between the transmitter and receiver so that only one antenna need be used. This switching is necessary because the high-power pulses of the transmitter would destroy the receiver if energy were allowed to enter the receiver.

Receiver: The receivers amplify and demodulate the received RF-signals. The receiver provides video signals on the output.

Radar Antenna: The Antenna transfers the transmitter energy to signals in space with the required distribution and efficiency. This process is applied in an identical way on reception.

Indicator: The indicator should present to the observer a continuous, easily understandable, graphic picture of the relative position of radar targets. The radar screen (in this case a PPI-scope) displays the echo signals in the form of bright spots called blips. The longer the pulses were delayed by the runtime, the further away from the centre of this radar scope they are displayed. The direction of the deflection on this screen is that in which the antenna is currently pointing.

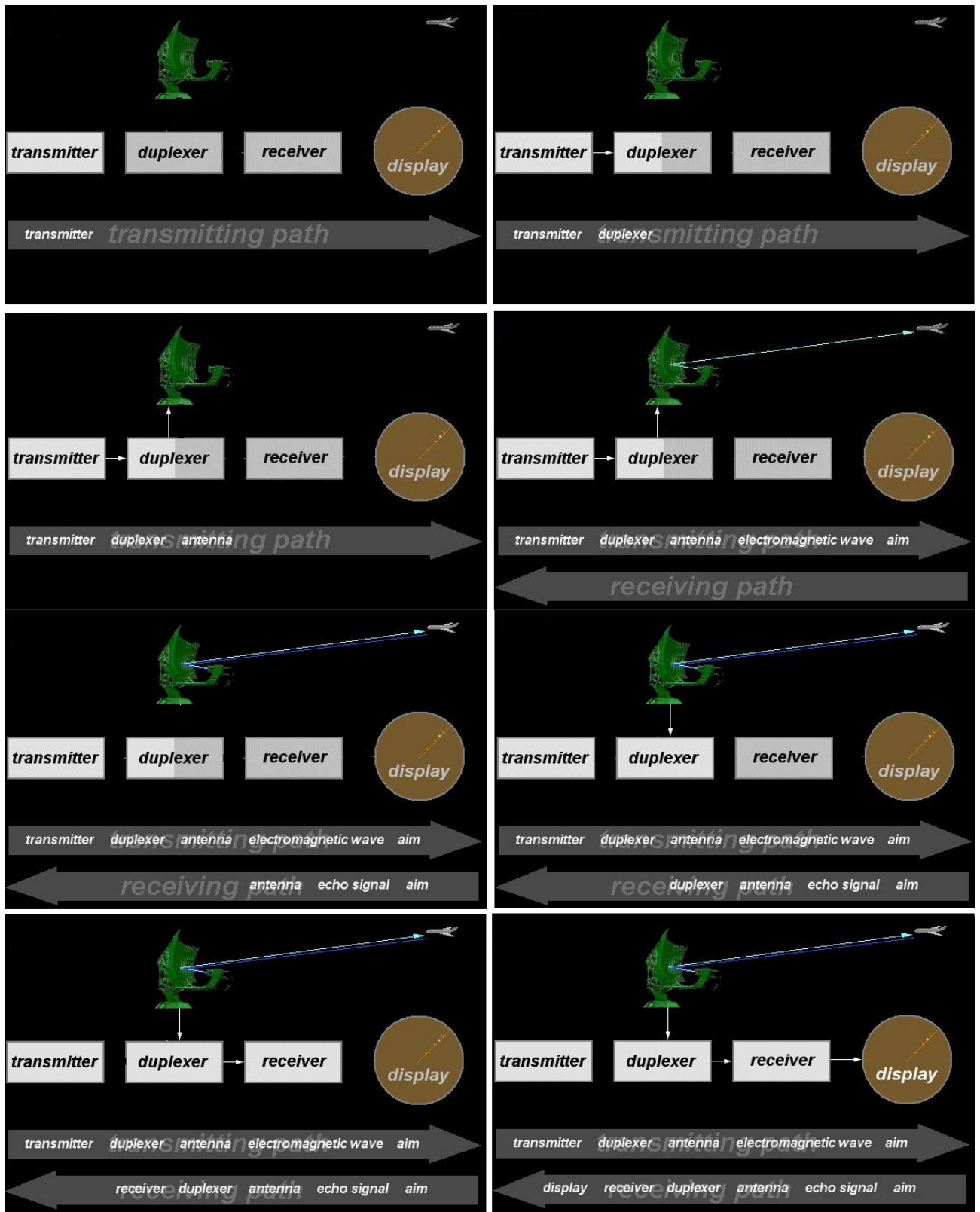


Figure 1.10. Step-by-step demonstration of basic processes involve in Radar

2. Radar Systems

In this chapter some details about Radar system is given. This discussion will elaborate the type of processing involved in that system and will help to understand what the limitations are in current electronic version of radar which can be handled in the optical version.

2.1. Classification of Radar System

Radar systems can be classified in term of Technologies and in term of Design. A brief detail of different radars has been mentioned so that we can reach to the conclusion that what has already been done, what else needed and which technology can be utilized to enhance the performance of radars.

2.1.1. Depending on Technologies

By technologies, in this perspective, mean that what type of signal processing is involved to realize radar to serve some purposes. Before going into the detail of different radar technologies, it is worth to mention an effect which is not only important in radar but also important in other fields like optics and acoustics. This effect is called as Doppler's Effect. In upcoming topic it will be seen that how much importance this effect possess in radar systems.

The Doppler's Effect:

The Doppler effect (or Doppler shift), named after Austrian physicist Christian Doppler who proposed it in 1842, is the difference between the observed frequency and the emitted frequency of a wave for an observer moving relative to the source of the waves. It is

commonly heard when a vehicle sounding a siren approaches, passes and recedes from an observer. The received frequency is higher (compared to the emitted frequency) during the approach, it is identical at the instant of passing by, and it is lower during the recession. This variation of frequency also depends on the direction the wave source is moving with respect to the observer; it is maximum when the source is moving directly toward or away from the observer and diminishes with increasing angle between the direction of motion and the direction of the waves, until when the source is moving at right angles to the observer, there is no shift. The Figure 2.1 shows the change in the frequency with respect to observers and source.



Figure 2.1. Frequency behaviour due to Doppler's effect

Let's try to represent this fact in mathematics with the perspective of radar. If R is the distance from the radar to target, the total number of wavelengths λ contained in the two-way path between the radar and the target is $2R/\lambda$. The distance R and the wavelength λ are assumed to be measured in the same units. Since one wavelength corresponds to an angular excursion of 2π radians, the total angular excursion Φ made by the electromagnetic wave during its transit to and from the target is $4\pi R/\lambda$ radians. If the target is in motion, R and the phase Φ are continually changing. A change in Φ with respect to time is equal to a frequency. This is the Doppler angular frequency ω_d [13] given by

$$\omega_d = 2\pi f_d = d\Phi/dt = (4\pi/\lambda)(dR/dt) = 4\pi v_r/\lambda$$

where f_d = Doppler frequency shift

v_r = relative velocity of target w.r.t radar

The Doppler frequency shift is

$$f_d = 2v_r/\lambda = 2v_r f_0/c \quad (2.1)$$

where f_0 = transmitted frequency

$$c = 3 \times 10^8 \text{ m/s}$$

There are four ways of producing the Doppler's effect. Radars may be coherent pulsed (CP), pulse-doppler radar, continuous wave (CW), or frequency modulated (FM). The earliest radar experiments were based on the continuous transmissions. The types of radar which involve continuous transmission are CW (continuous wave) and FM-CW (frequency modulated – continuous wave).

2.1.1.1. Continuous Wave (CW) Radar

The study of CW radar serves better to understand the nature and use of Doppler information contained in the echo signal. The CW radar provides a measurement of relative velocity which may be used to distinguish moving targets from stationary objects or clutter. Clutter refers to radio frequency (RF) echoes returned from targets which are uninteresting to the radar operators. In addition, this type of radar has many interesting applications, which will be presented.

A simple CW radar is shown in the below block diagram, Figure 2.2. A continuous (un-modulated) signal of frequency ' f_0 ' has been generated by transmitter and radiated by antenna. The portion of radiated energy, after intercepting from target, scattered in the different direction and some of it scattered back in the direction of radar. The back scattered signal is collected by the receiving antenna (in this case same as transmitted antenna). If the target is in motion with some velocity, relative to the radar, the received signal will be shifted in frequency from the transmitted frequency f_0 by an amount "+" or "-" f_d as given by Eq. (2.1). The plus sign associated with the Doppler frequency applies if the distance between target and radar is decreasing (closing target), that is, when the

received signal frequency is greater than the transmitted signal frequency. The minus sign applies if the distance is increasing (receding target). The received echo signal at a frequency $f \pm f_d$ enters the radar via the antenna and is heterodyned in the detector (mixer) with a portion of the transmitter signal f_0 to produce a Doppler beat note of frequency f_d [13]. The sign of f_d is lost in this process.

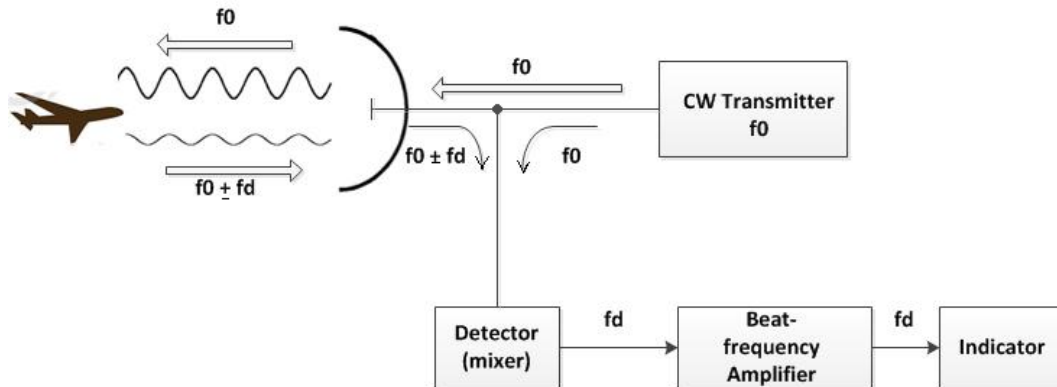


Figure 2.2. Block Diagram of CW radar

A single antenna serves the purpose of transmission and reception in the simple CW radar described above. In principle, a single antenna may be employed since the necessary isolation between the transmitted and the received signals is achieved via separation in frequency as a result of the Doppler effect. In practice, it is not possible to eliminate completely the transmitter leakage. However, transmitter leakage is not always undesirable. A moderate amount of leakage entering the receiver along with the echo signal supplies the reference necessary for the detection of the Doppler frequency shift. If a leakage signal of sufficient magnitude were not present, a sample of the transmitted signal would have to be deliberately introduced into the receiver (as shown in above figure) to provide the necessary reference frequency.

The amount of isolation between transmitted and received signals depends on the transmitter power and the accompanying transmitter noise as well as the sensitivity of the receiver. Additional isolation requires in the CW long-range radar because of high transmitted power and receiver sensitivity. Moreover, the amount of isolation in long-range CW radar is more often determined by the noise that accompanies the transmitter leakage signal rather than by any damage caused by high power. The largest isolations are obtained with two antennas-one for transmission, the other for reception-physically separated from one

another. The more directive the antenna beam and the greater the spacing between antennas, the greater will be the isolation [13].

Intermediate-frequency receiver: The receiver of the simple CW radar of Figure 2.2 is in some respects analogous to a super-heterodyne receiver. Receivers of this type are called homodyne receivers, or super-heterodyne receivers with zero IF. The function of the local oscillator is replaced by the leakage signal from the transmitter. Such a receiver is simpler than one with a more conventional intermediate frequency since no IF amplifier or local oscillator is required. However, the simpler receiver is not as sensitive because of increased noise at the lower intermediate frequencies caused by flicker effect. Flicker-effect noise occurs in semiconductor devices such as diode detectors and cathodes of vacuum tubes. The noise power produced by the flicker effect varies with frequency. This is in contrast to shot noise or thermal noise, which is independent of frequency. Thus, at the lower range of frequencies (audio or video region), where the Doppler frequencies usually are found, the detector of the CW receiver can introduce a considerable amount of flicker noise, resulting in reduced receiver sensitivity. For short-range, low-power, applications this decrease in sensitivity might be tolerated since it can be compensated by a modest increase in antenna aperture and/or additional transmitter power. But for maximum efficiency with CW radar, the reduction in sensitivity caused by the simple Doppler receiver with zero IF cannot be tolerated.

The effects of flicker noise are overcome in the normal super-heterodyne receiver by using an intermediate frequency high enough to render the flicker noise. Figure 2.3 below shows a block diagram of the CW radar whose receiver operates with a nonzero IF. Separate antennas are shown for transmission and reception instead of the usual local oscillator found in the conventional super-heterodyne receiver, the local oscillator (or reference signal) is derived in this receiver from a portion of the transmitted signal mixed with a locally generated signal of frequency equal to that of the receiver IF. Since the output of the mixer consists of two sidebands on either side of the carrier plus higher harmonics, a narrowband filter selects one of the sidebands as the reference signal. The improvement in receiver sensitivity with an intermediate-frequency super-heterodyne might be as much as 30 dB over the simple receiver of Figure 2.3.

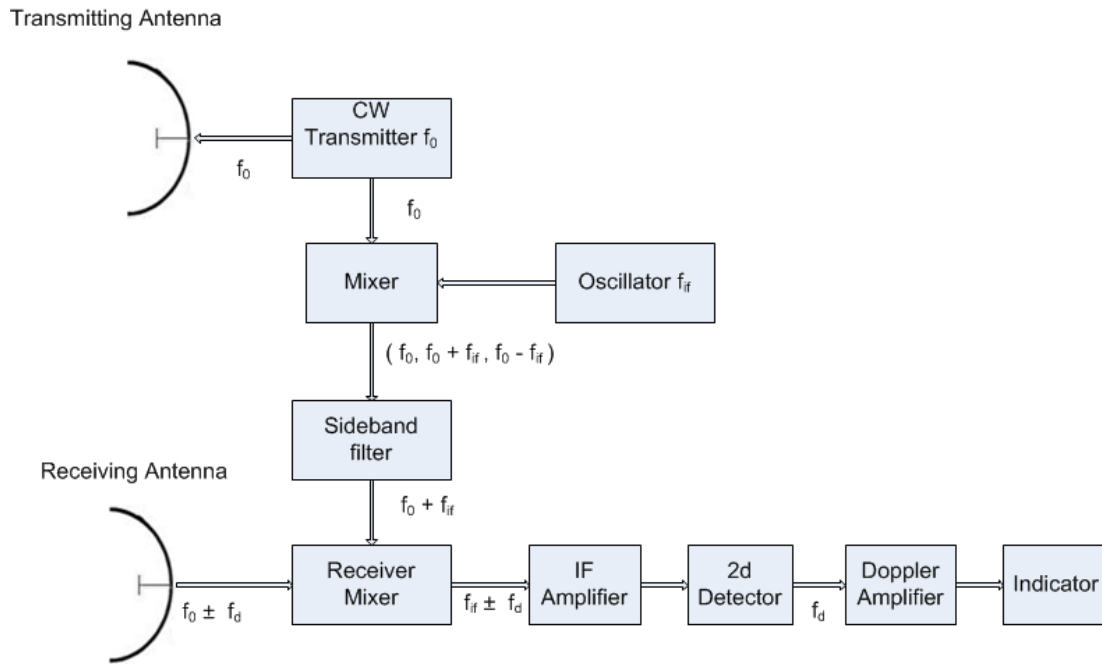


Figure 2.3. Block diagram of CW radar with nonzero IF receiver

One of the greatest shortcomings of the simple CW radar is its inability to obtain a measurement of range which is related to the relatively narrow spectrum (bandwidth) of its transmitted waveform. It lacks the timing mark necessary to allow the system to time accurately the transmit and receive cycle and convert the measured round-trip-time into range. This limitation can be overcome by modulating the CW carrier, as in the frequency-modulated radar described next.

2.1.1.2. Frequency Modulated CW (FMCW) Radar

The spectrum of a CW transmission can be broadened by the application of modulation, which can be amplitude, frequency, or phase. An example of an amplitude modulation is the pulse radar. The narrower the pulse, the more accurate the measurement of range and the broader the transmitted spectrum [13]. A widely used technique to broaden the spectrum of CW radar is to frequency-modulate the carrier. The timing mark, for range measurement, is the changing frequency. The transit time is proportional to the difference in frequency between the echo signal and the transmitted signal.

A block diagram illustrating the principle of the FM-CW radar is shown in Figure 2.4 below. A portion of the transmitter signal acts as the reference signal required to produce the

beat frequency when heterodyned. It is introduced directly into the receiver via a cable or other direct connection.

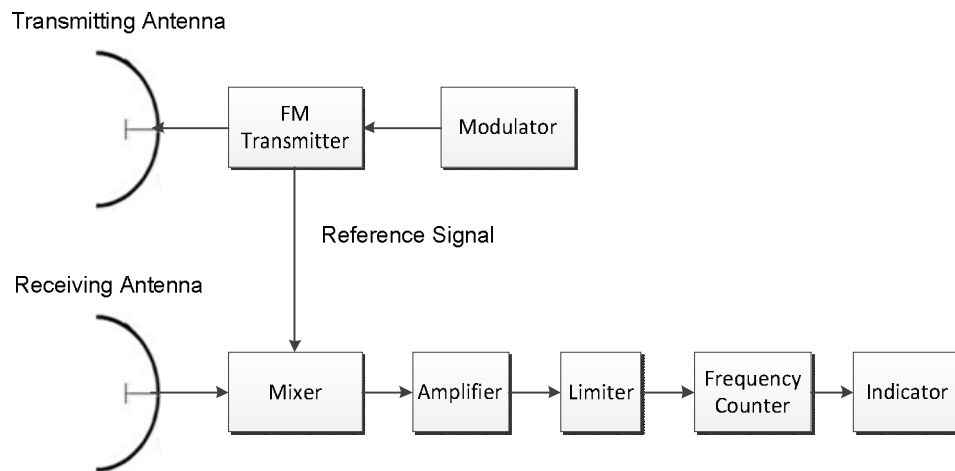


Figure 2.4, Block diagram of FM-CW radar

Ideally, the isolation between transmitting and receiving antennas is made sufficiently large so as to reduce the transmitter leakage signal, which arrives at the receiver via the coupling between antennas, to a negligible level. The beat frequency is amplified and limited to remove any amplitude fluctuations. The frequency of the amplitude-limited beat note is measured with a cycle-counting frequency meter calibrated in distance.

Range and Doppler measurement: Assume that the transmitter frequency increases linearly with time, as shown by the solid line in Figure 2.5. If there is a reflecting object at a distance R , an echo signal will return after a time $T = 2R/c$. The dashed line in the Figure 2.5 represents the echo signal. If the echo signal is heterodyned with a portion of the transmitter signal in a nonlinear element such as a diode, a beat note f_b will be produced. If there is no Doppler frequency shift, the beat note (difference frequency) is a measure of the target's range and $f_b = f_r$, where f_r is the beat frequency due only to the target's range. If the rate of change of the carrier frequency f_0 the beat frequency is

$$f_r = f_0 T = 2R f_0/c$$

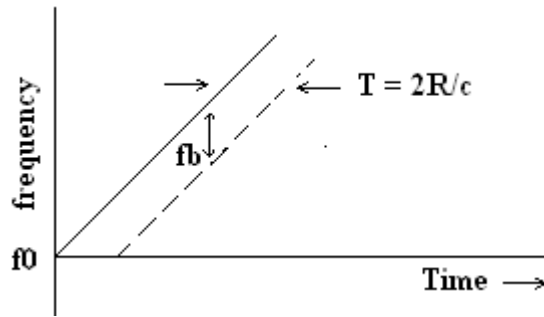


Figure 2.5. Linear Frequency Modulation

In any practical CW radar, the frequency cannot be continually changed in one direction only. Periodicity in the modulation is necessary, like the modulation can be in triangular, saw-tooth, sinusoidal, or some other shape. If the frequency is modulated at a rate f_m over a range Δf the beat frequency is

$$f_r = (2R/c)2f_m \quad \Delta f = 4Rf_m \Delta f/c \quad (2.2)$$

Thus the measurement of the beat frequency determines the range R .

As mentioned in the previous topic, simple CW radar can be used to measure target speed through the Doppler shift. FM-CW radar also ends up being affected by the Doppler shift, which creates an ambiguity. Suppose the FM-CW radar isn't moving and it's generating a ramp of rising frequencies. If it transmits a particular frequency at a certain time, then when it receives an echo after a specific delay time with the same frequency there is no ambiguity. The round-trip time of the signal is just the measured delay, and the range is easy to calculate.

However, if the FM-CW radar is moving ahead, as it might be expected to if it's installed in an aircraft and pointed forward to the ground, then the Doppler shift will drive up the frequency of the return. If the return signal comes back with a particular frequency, it's actually a Doppler-shifted return from a transmission at a lower frequency, and the range is actually greater than would be expected from the delay time between transmission and reception of the same frequency. Of course, if the FM-CW radar was moving backward the return would be shifted down in frequency and the range would be shorter, but aircraft do not fly backwards in normal operation.

The way around this is to generate the ramp of frequencies up and down in a triangular fashion. To show how this works, let's assume again that the FM-CW radar is stationary and compare the frequency-versus-time plot for transmit and receive, along with a plot of the difference between the two:

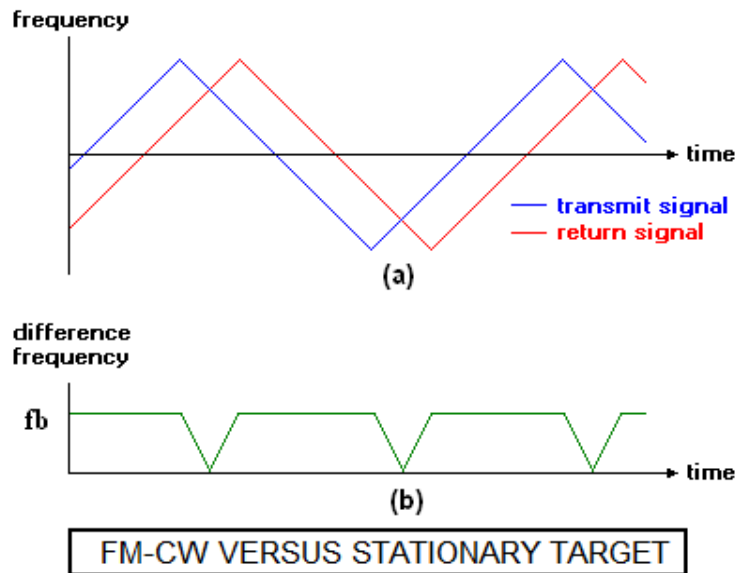


Figure 2.6. (a) Triangular frequency modulation, (b) beat note of (a) for stationary FM-CW radar

As the illustration in Figure 2.6 above shows, for a stationary FM-CW radar the return signal tracks the transmit signal perfectly, returning with a fixed delay. Notice that at any single time on the plot there is a constant difference between the transmit and receive frequencies, except for the short window between the time the transmit signal changes direction and receive signal follows.

Now let's put the FM-CW radar into forward motion and create the same plot. The return from stationary target is rendered in light gray in below Figure 2.7 to provide a reference.

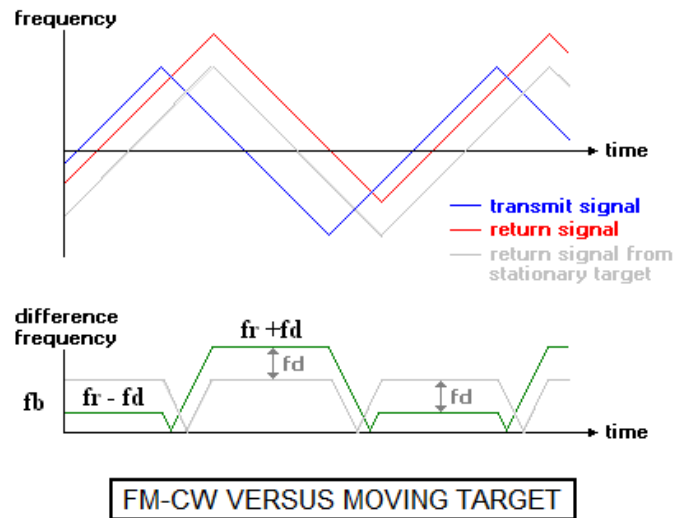


Figure 2.7. Moving FM-CW radar

The Doppler shift creates a distinctive offset between the transmit signal and the receive signal. This is because on the rising half of the ramp the transmit frequency is increasing and the increased Doppler-shifted return signal is "catching up" with the changing transmit signal, but on the falling half of the ramp the transmit signal is decreasing and the increased Doppler-shifted receive signal is "lagging behind" the changing transmit signal.

This means the difference between the transmit and receive frequencies is small on the rising half of the ramp, and large on the falling half of the ramp. FM-CW radar can use this difference to determine both range and speed. Since the Doppler-shifted component is subtracted on the rising half of the ramp and added on the falling half of the ramp, the range is given by the average difference of the two cycles i.e. $1/2[f_b(\text{up}) + f_b(\text{down})] = f_r$.

$$f_b(\text{up}) = f_r - f_d$$

$$f_b(\text{down}) = f_r + f_d$$

This average can be subtracted from the difference in the second half of the cycle to give the Doppler-shifted velocity component, given as " f_d " in the Figure 2.7. The FM-CW radar principle is used in the aircraft radio altimeter to measure height above the surface of the earth.

2.1.1.3. Bistatic Radar Set

Generally, the transmitter and receiver share a common antenna, which is called a monostatic radar system. A bistatic radar consists of separately located (by a considerable distance) transmitting and receiving sites as shown in Figure 2.8. Therefore, a monostatic Doppler radar can be upgraded easily with a bistatic receiver system or (by use of the same frequency) two monostatic radars are working like a bistatic radar. A bistatic radar makes use of the forward scattering of the transmitted energy.

In case of a bistatic radar set there is a larger distance between the transmitting unit and the receiving unit and usually a greater parallax. This means, a signal can also be received when the geometry of the reflecting object reflects very little or no energy (stealth technology) in the direction of the monostatic radar.

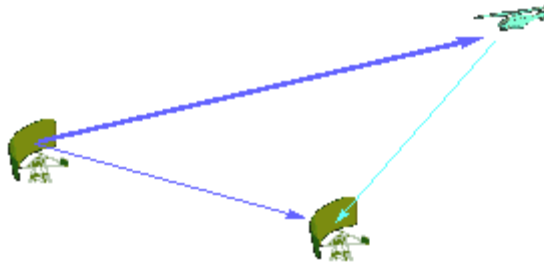


Figure 2.8. Bistatic Radar separate transmitter and receiver

In practice it is mainly used for weather radar. This system is also of some importance in military applications. The so called “semi-active” missile control system, as used in the missile unit “HAWK” is practically a bistatic radar.

By receiving the side lobes of the transmitting radars direct beam, the receiving sites radar can be synchronized. If the main lobe is detected, an azimuth information can be calculated also. A number of specialized bistatic systems are in use, for example, where multiple receiving sites are used to correlate target position.

2.1.1.4. Moving Target Indication (MTI) Radar

The Doppler frequency shift produced by a moving target may be used in pulse radar just as in the CW radar discussed above, to determine the relative velocity of a target or to separate desired moving targets from undesired stationary objects (clutter). The use of

Doppler to separate small moving targets in the presence of large clutter has probably been of far greater interest. MTI radar is pulse radar that utilizes the Doppler frequency shift to discriminate moving targets from the fixed ones.

MTI is a necessity in high-quality air-surveillance radars that operate in the presence of clutter. Its design is more challenging than that of simple pulse radar or simple CW radar. In principle, the CW radar may be converted into a pulse radar as shown in the Figure 2.9 by providing a power amplifier and a modulator to turn the amplifier on and off for the purpose of generating pulses. In case of pulse radar as shown below a small portion of the CW oscillator power that generates the transmitted pulses is diverted to the receiver to take the place of the local oscillator. This CW signal acts as a replacement for the local oscillator as well as coherent (will be explained later) reference needed to detect the Doppler frequency shift.

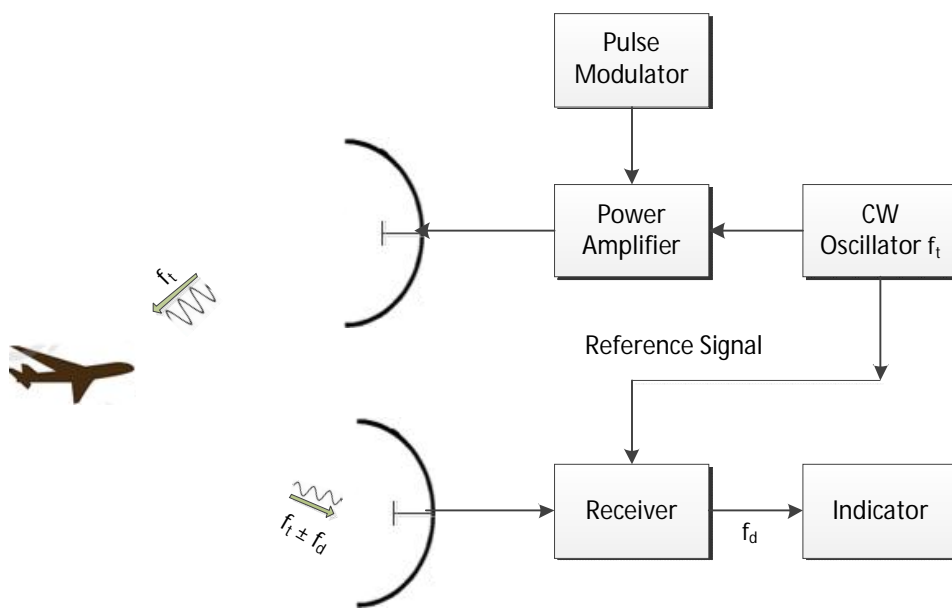


Figure 2.9.MTI radar block diagram

If the CW oscillator voltage is represented as $A_1 \sin 2\pi f_t t$, where A_1 is the amplitude and f_t the carrier frequency, the reference signal is

$$V_{\text{ref}} = A_2 \sin 2\pi f_t t$$

And the Doppler-shifted echo signal voltage is

$$V_{\text{echo}} = A_3 \sin [2\pi(f_t \pm f_d)t - 4\pi f_t R_0/c]$$

where A_2 = Amplitude of reference signal

A_3 = Amplitude of signal received from target at range R_0

f_d = Doppler frequency shift

t = time, c = velocity of propagation

The reference signal and the target echo signal are heterodyned in the mixer stage of the receiver. Only the low-frequency (difference-frequency) component from the mixer is of interest and voltage is given by

$$V_{\text{diff}} = A_4 \sin (2\pi f_d t - 4\pi f_t R_0/c) \quad (2.3)$$

For stationary targets the Doppler frequency shift will be zero; hence V_{diff} will not vary with time and may take on any constant value from $+A_4$ to $-A_4$, including zero. However, when the target is in motion relative to the radar, f_d has a value other than zero and the voltage corresponding to the difference frequency from the mixer Eq. (2.3) will be a function of time [13].

The simple MTI radar shown in Figure 2.9 above is not the most typical. The block diagram of more common MTI radar employing a power amplifier is shown in Figure 2.10 below and the difference is the way in which the reference signal is generated. The coherent reference is supplied by an oscillator called the *coho*, as shown in the Figure, which stands for coherent oscillator. The coho is a stable oscillator whose frequency is the same as the intermediate frequency used in the receiver. In addition to providing the reference signal, the output of the coho f_c is also mixed with the local-oscillator frequency f_l . The local oscillator must also be a stable oscillator and is called *stalo*. The RF echo signal is heterodyned with the stalo signal to produce the IF signal just as in the conventional super-heterodyned receiver.

The characteristic feature of coherent MTI radar is that the transmitted signal must be coherent (in phase) with the reference signal in the receiver. This is accomplished in the radar system by generating the transmitted signal from the coho reference signal. The function of the stalo is to provide the necessary frequency translation from the IF to the transmitted (RF) frequency. Although the phase of the stalo influences the phase of the transmitted signal, any

stalo phase shift is cancelled on reception because the stalo that generates the transmitted signal also acts as the local oscillator in the receiver. The reference signal from the coho and the IF echo signal are both fed into a mixer called the phase detector. The phase detector differs from the normal amplitude detector since its output is proportional to the phase difference between the two input signals.

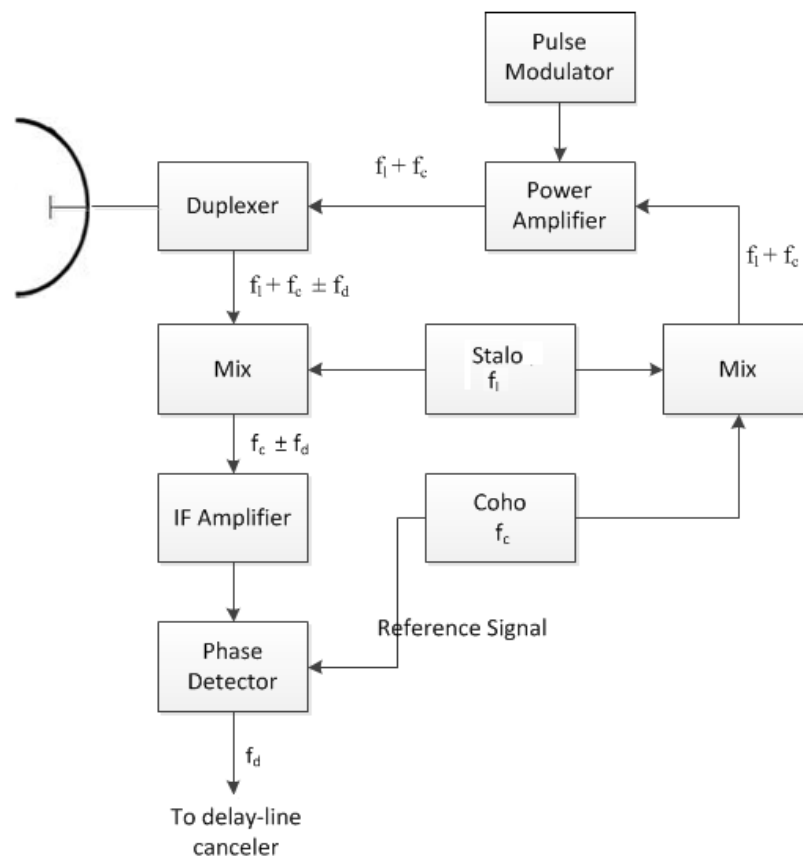


Figure 2.10. Block diagram of more common MTI radar

The delay-line canceler acts as a filter to eliminate the d-c component of fixed targets and to pass the a-c components of moving targets i-e to separate fixed targets from moving ones.

Simple MTI using analog technology is a straightforward idea, but it's not very sophisticated; it results in a signal that is noisy and difficult to interpret. A more sophisticated scheme is the "Ground Moving Target Indicator (GMTI)", discussed below.

One of the problems with MTI as described is that it won't work if the radar platform is moving, since then the clutter returns will be very different from pulse to pulse and won't cancel out.

A trick was developed that could be used to make a radar carried in an aircraft look like it is standing still, at least from one pulse to the next. Suppose an aircraft has two radar antennas in tandem and is taking radar observations to the side of the aircraft flight track. The leading antenna emits a pulse, then advances forward and picks up the return. When the trailing antenna reaches the position where the leading antenna was when it emitted its pulse, the trailing antenna emits its own pulse, and then advances to pick the return in the same position as did the leading antenna. This gives two pulses and returns obtained in the same location, allowing a clutter canceler to be used to compare them to find moving targets.

2.1.1.5. Pulse Doppler Radar

Pulse radar that extracts the Doppler frequency shift for the purpose of detecting moving targets in the presence of clutter is either MTI radar or a pulse Doppler radar. The distinction between them is based on the fact that in a sampled measurement system like pulse radar, ambiguities can arise in both the Doppler frequency (relative velocity) and the range (time delay) measurements. Range ambiguities are avoided with a low sampling rate (low pulse repetition frequency (PRF)), and Doppler frequency ambiguities are avoided with a high sampling rate. However, in most radar applications the sampling rate, or PRF, cannot be selected to avoid both types of measurement ambiguities. Therefore a compromise must be made and the nature of the compromise generally determines whether the radar is called an MTI or a pulse doppler. MTI usually refers to a radar in which the PRF is chosen low enough to avoid ambiguities in range (no multiple-time-around echoes) but with the consequence that the frequency measurement is ambiguous and results in blind speeds. Those relative target velocities which result in zero MTI response are called blind speeds and it also one of the limitations of MTI radar. The pulse doppler radar, on the other hand, has a high pulse repetition frequency that avoids blind speeds, but it experiences ambiguities in range.

2.1.1.6. Pulse Compression in Radar

As mentioned in last section, there is a trade-off in determining pulse width. A short pulse gives better range accuracy, but it also means less energy dumped out to sense a target.

Pulse Doppler makes the matter worse: interpreting the Doppler shift from a short pulse is harder than interpreting the shift from a long pulse, and so a short pulse gives poorer velocity resolution. A modern improvement in radar is known as "pulse compression" which is the answer of above mentioned problem.

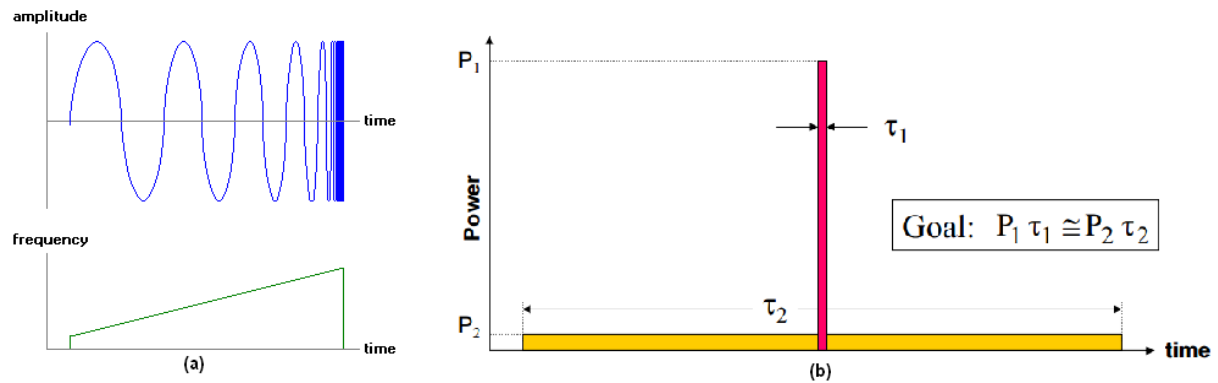


Figure 2.11.(a) Pulse Compression chirp Waveform, (b) Simplified view of concept

In the simplest form it amounts to generating the pulse as a frequency-modulated ramp or "chirp", rising from a low frequency to a high frequency as shown in above Figure 2.11 (a). This increases the energy of the pulse (wave energy increases with frequency) and permits much less ambiguity in Doppler interpretation. Essentially, pulse compression trades bandwidth for pulse length, and pulse compression schemes are rated by a "compression factor" given by:

$$\text{compression_factor} = \text{chirp_range} * \text{pulse duration}$$

Figure 2.11 (b) shows the simplified view of pulse compression concept. Energy content of long-duration, low-power pulse will be comparable to that of the short-duration, high-power pulse

$$\tau_1 \ll \tau_2 \text{ and } P_1 \gg P_2$$

There are also "coded" schemes for pulse compression that involve shifting parts of the pulse in phase. For example, consider a simple sine wave, going through cycle after cycle, with each cycle consisting of the signal going from zero amplitude to a positive value back through zero to a negative value and back to zero again. A normal sine wave will go through identical cycles in sequence, varying from positive to negative through each cycle.

Now suppose that every third cycle the sine wave is inverted in polarity, varying from negative to positive instead of positive to negative, or in other words shifted 180 degrees in phase, Figure 2.12:

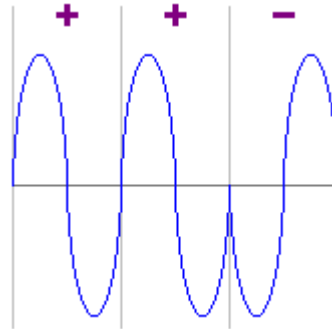


Figure 2.12. Binary Phase Modulation

The three-part pattern of un-shifted and shifted cycles can be described in a simple shorthand as a type of "binary code", with values of "+" (un-shifted) and "-" (shifted). In this case the code is given by:

+ + -

In any case, by Fourier analysis the abrupt transition from a "+" cycle to a "-" cycle involves a very wide spectrum of Fourier components, and so by the seemingly simple change of inverting one cycle of polarity results in a compressed high-bandwidth pulse generated from a relatively low-bandwidth signal. Of course, the received return pulse is processed by summing the echoes obtained from the three pulses, with the third cycle returned to normal polarity in the summation. This, by a bit of signal processing magic, gives an energetic return even with a short pulse. There are various types of coding sequences, each with somewhat different properties, and some use other phase shifts than 180 degrees.

2.1.2. Depending on Design

2.1.2.1. Air-Defence Radars

Air-Defence Radars can detect air targets and determine their position, course, and speed in a relatively large area. The maximum range of Air-Defence Radar can exceed 300 miles, and the bearing coverage is a complete 360-degree circle. Air-Defence Radars are

usually divided into two categories, based on the amount of position information supplied. Radar sets that provide only range and bearing information are referred to as two-dimensional, or *2D, radars*. Radar sets that supply range, bearing, and height are called three-dimensional, or *3D, radars*.

Air-Defence Radars are used as early-warning devices because they can detect approaching enemy aircraft or missiles at great distances. In case of an attack, early detection of the enemy is vital for a successful defence against attack. Anti-aircraft defences in the form of anti-aircraft artillery, missiles, or fighter planes must be brought to a high degree of readiness in time to repel an attack. Range and bearing information, provided by Air-Defence Radars, used to initially position a fire-control tracking radar on a target.

Another function of the Air-Defence Radar is guiding combat air patrol (CAP) aircraft to a position suitable to intercept an enemy aircraft. In the case of aircraft control, the guidance information is obtained by the radar operator and passed to the aircraft by either voice radio or a computer link to the aircraft. Major Air-Defence Radar Applications are:

- Long-range early warning (including airborne early warning, AEW)
- Ballistic missile warning and acquisition
- Height-finding
- Ground-controlled interception (GCI)

2.1.2.2. Air Traffic Control (ATC)-Radars

The following Air Traffic Control (ATC) surveillance, approach and landing radars are commonly used in Air Traffic Management (ATM):

- En-route radar systems,
- Air Surveillance Radar (ASR) systems,
- Precision Approach Radar (PAR) systems,
- Surface movement radars, and
- Special weather radars.

En-Route Radars

En-route radar systems operate in L-Band usually. These radar sets initially detect and determine the position, course, and speed of air targets in a relatively large area up to 250 nm (nautical miles).



Figure 2.13.SRE-M7, typically en-route radar made by the German DASA company

Air Surveillance Radar (ASR)

Airport Surveillance Radar (ASR) is an approach control radar used to detect and display an aircraft's position in the terminal area. These radar sets operate usually in E-Band, and are capable of reliably detecting and tracking aircraft at altitudes below 25,000 feet (7,620 meters) and within 40 to 60 nm (75 to 110 km) of their airport.



Figure 2.14.The Air Surveillance Radar ASR-12

Precision Approach Radar (PAR)

The ground-controlled approach is a control mode in which an aircraft is able to land in bad weather. The pilot is guided by ground control using precision approach radar. The guidance information is obtained by the radar operator and passed to the aircraft by either voice radio or a computer link to the aircraft.



Figure 2.15.Precision Approach Radar PAR-80 made by ITT

Surface Movement Radar (SMR)

The Surface Movement Radar (SMR) scans the airport surface to locate the positions of aircraft and ground vehicles and displays them for air traffic controllers in bad weather. Surface movement radars operate in J- to X- Band and use an extremely short pulse-width to provide an acceptable range-resolution.



Figure 2.16. Surface Movement Radar ASDE

Specially weather-radar applications

Weather radar is very important for the air traffic management. There are weather-radars specially designed for the air traffic safety.



Figure 2.17. Microburst radar MBR

Before going into discussion of radar devices, a very important concept related to radar should be discussed. This concept deal is all about the coherence and non-coherence processing in radars.

2.2. Coherent and Non-coherent Processing in Radars

Coherent radar signal processing (i.e., processing that uses the phase or frequency of the transmitted and received signals) could be used to discriminate moving targets from weather and other types of background clutter. A coherent radar compares the phase or frequency of a target echo with a stable oscillator or reference signal source. Natural objects, such as trees or islands, tend to be relatively steady in phase or frequency [1]. (An important exception is the Doppler-shifted frequency of echoes from weather phenomena.) However,

moving targets such as aircraft or ships cause echoes that vary compared with the stable source. MTI and the pulse-doppler radars make use of coherent processing to recognize the doppler component produced by a moving target. In these systems, amplitude fluctuations are removed by the phase detector. The operation of this type of radar depends upon a reference signal at the radar receiver that is coherent with the transmitter signal.

It is also possible to use the amplitude fluctuations to recognize the doppler component produced by a moving target. Radar which uses amplitude instead of phase fluctuations is called non-coherent. The non-coherent radar does not require an internal coherent reference signal or a phase detector as does the coherent require.

2.3. Radar Devices

In the coming discussion some of the devices like antenna etc. will not be discussed because the focus will only be on those devices which will help to establish the point of limitations well.

2.3.1. Transmitter

The radar transmitter produces the short duration high-power RF pulses of energy that are radiated into space by the antenna. The radar transmitter is required to have the following technical and operating characteristics:

- The transmitter must have the ability to generate the required mean RF power and the required peak power which can affect the range and ultimately the resolution of radar.
- The transmitter must have a suitable RF bandwidth.
- The transmitter must have a high RF stability to meet signal processing requirements.
- The transmitter must be easily modulated to meet waveform design requirements.
- The transmitter must be efficient, reliable and easy to maintain and the life expectancy and cost of the output device must be acceptable.

There is no one universal transmitter best suited for all radar applications. Each power generating device has its own particular advantages and limitations that require the radar

system designer to examine carefully all the available choices when configuring a new radar design. Radar transmitters can be classified in term of coherent (low power RF oscillator) and non-coherent (high power RF oscillator) given as:

- One main type of transmitters is the *keyed-oscillator* type [12]. In this transmitter one stage or tube, usually a magnetron produces the RF pulse. The oscillator tube is keyed by a high-power dc pulse of energy generated by a separate unit called the modulator. This transmitting system is called **POT (Power Oscillator Transmitter)**. Radar units fitted with a POT are either non-coherent or pseudo-coherent.
- **Power-Amplifier-Transmitters (PAT)** [12] is used in many recently developed radar sets. In this system the transmitting pulse is caused from a waveform generator. It is taken to the necessary power with an amplifier following (Amplitron, Klystron or Solid-State-Amplifier). Radar units fitted with a PAT are fully coherent in the majority of cases.

2.3.1.1. Pseudo-coherent or Non-coherent Radar

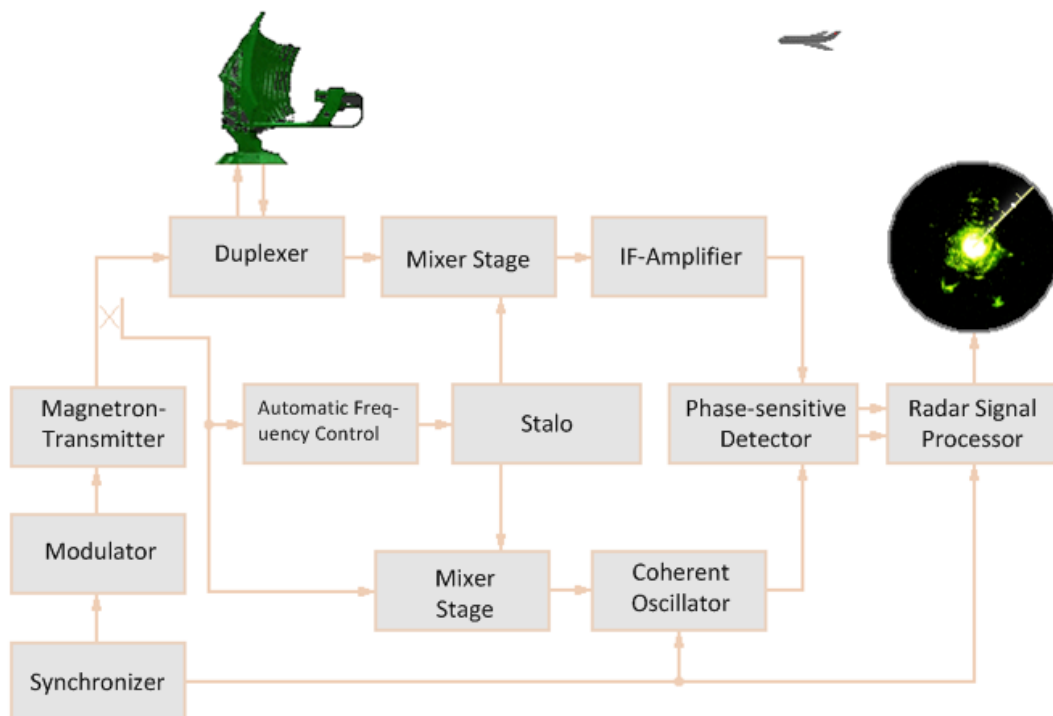


Figure 2.18. Block diagram of pseudo-coherent radar

Magnetron Oscillator:

The physical structure of magnetron is shown below in the Figure 2.19. The anode of a magnetron is fabricated into a cylindrical solid copper block. The cathode and filament are at the centre of the tube and are supported by the filament leads. The filament leads are large and rigid enough to keep the cathode and filament structure fixed in position. The cathode is indirectly heated and is constructed of a high-emission material. The 8 up to 20 cylindrical holes around its circumference are resonant cavities. The cavities control the output frequency. A narrow slot runs from each cavity into the central portion of the tube dividing the inner structure into as many segments as there are cavities. The open space between the plate and the cathode is called the interaction space. In this space the electric and magnetic fields interact to exert force upon the electrons. The magnetic field is usually provided by a strong, permanent magnet mounted around the magnetron so that the magnetic field is parallel with the axis of the cathode.

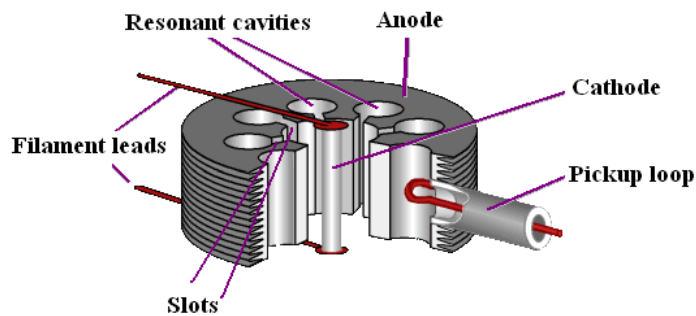


Figure 2.19. Physical structure of Magnetron

Basic Operation: The production of microwave frequencies can be divided into four phases.

1. Production and acceleration of electron beam
2. Velocity Modulation of electron beam
3. Forming of “Space Charge Wheel”
4. Dispense Energy to the ac field

The detail of the whole operation to generate RF is out of the scope of this document.

Each transient oscillation in magnetron occurs with a random phase i-e without a predictable phase. So, the transmitting pulses that are generated by a magnetron are therefore

not coherent and mostly used in non-coherent or pseudo-coherent radar (coherent-on-receive radar). However, injection locking can be used to allow a magnetron based transmitter to emulate coherent operation. In injection locking, a signal is injected into the output of the magnetron prior to pulsing the tube. This microwave signal causes the energy build-up within the tube to concentrate at the frequency of the injected signal and also to be in phase with it. If the injected signal is coherent with the local oscillator (LO) of the receiver, the resulting transmitted signal is also coherent with the receiver LO and hence the resulting radar system can measure the relative phase on receive, providing coherent operation. The degree of coherency is generally not as good as with an actual coherent amplifier chain, but such transmitters can be substantially cheaper than fully coherent systems.

Modulator

Radio frequency energy in radar is transmitted in short pulses with time durations that may vary from 1 to 50 microseconds or more. A special modulator is needed to produce this impulse of high voltage. The hydrogen thyratron modulator, Figure 2.18, is the most common radar modulator. It employs a pulse-forming network (PFN), as shown in the figure below, that is charged up slowly to a high value of voltage. The network is discharged rapidly through a pulse transformer by the thyratron keyer tube to develop an output pulse. The shape and duration of the pulse are determined by the electrical characteristics of the PFN and of the pulse transformer.

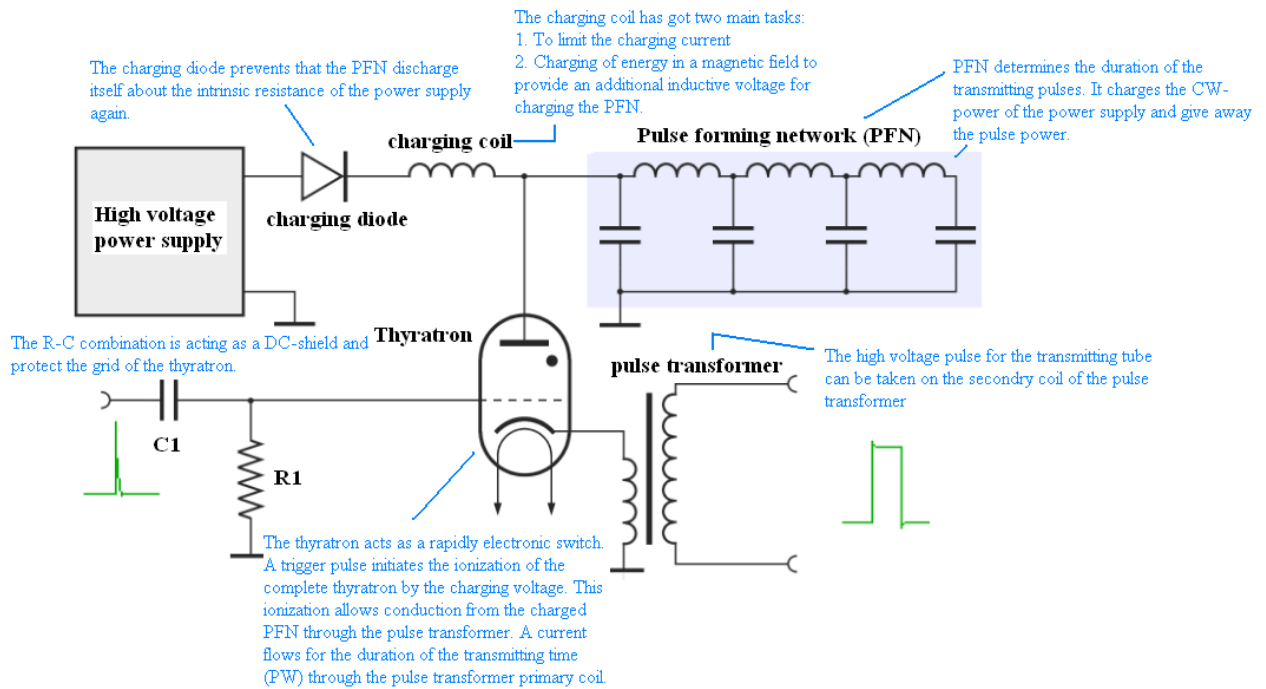


Figure 2.18. Thyatron Modulator

As circuit for storing energy the thyatron modulator uses essentially a short section of artificial transmission line which is known as the PFN. Via the charging path this PFN is charged on the double voltage of the high voltage power supply with help of the magnetic field of the charging impedance. Simultaneously this charging impedance limits the charging current. The charging diode prevents that the PFN discharge himself about the intrinsic resistance of the power supply again.

The function of thyatron is to act as an electronic switch which requires a positive trigger of only 150 volts. The thyatron requires a sharp leading edge for a trigger pulse and depends on a sudden drop in anode voltage (controlled by the pulse-forming network) to terminate the pulse and cut off the tube. The R-C Combination acts as a DC-shield and protects the grid of the thyatron. This trigger pulse initiates the ionization of the complete thyatron by the charging voltage. This ionization allows conduction from the charged PFN through pulse transformer. The output pulse is then applied to an oscillating device, such as a magnetron.

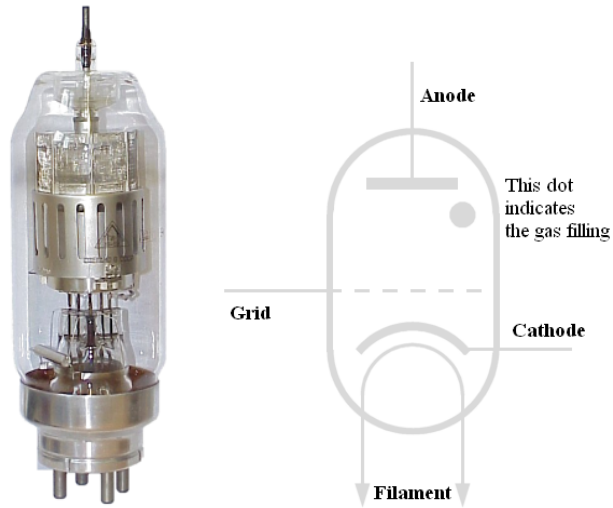


Figure 2.19. Thyatron and its symbol

2.3.1.2. Coherent Radar

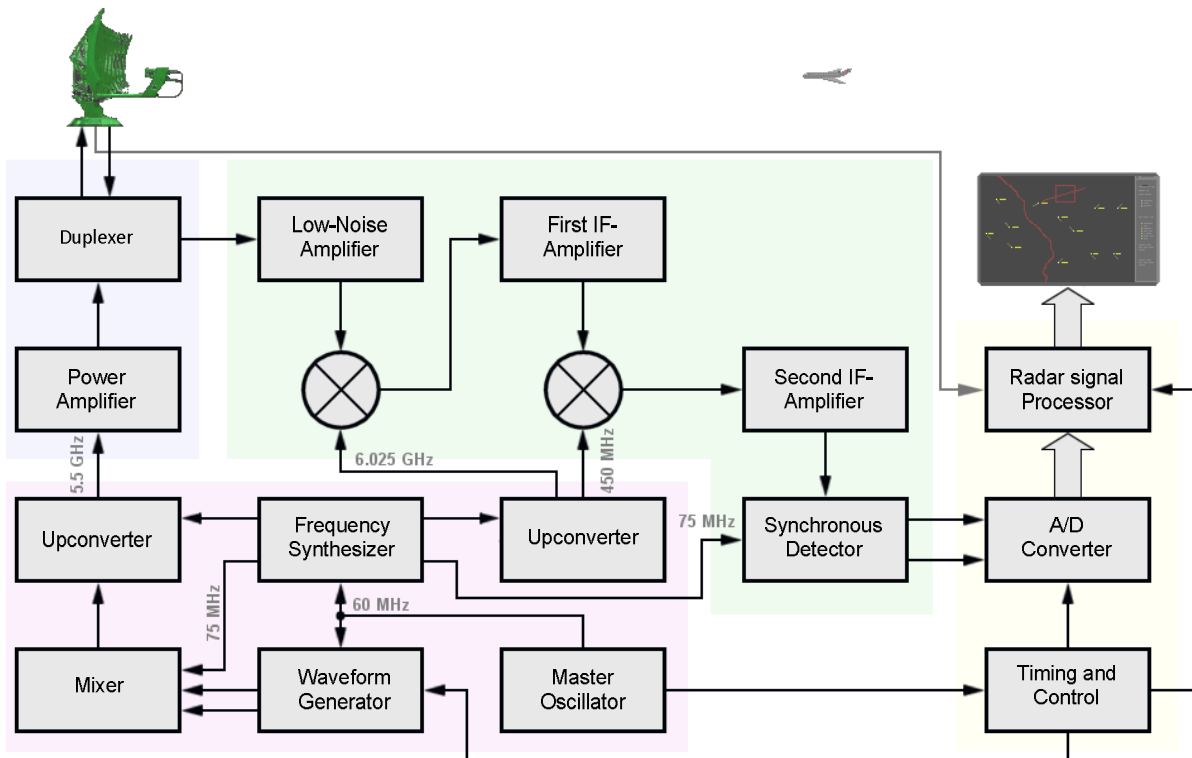


Figure 2.20. Block diagram of fully coherent radar

The block diagram Figure 2.20 above illustrates the principle of fully coherent radar. The fundamental feature is that all signals are derived at low level and the output device serves only as an amplifier. All the signals are generated by one master timing source, usually a synthesiser, which provides the optimum phase coherence for the whole system. The output device would typically be a klystron, TWT or solid state.

Klystron Amplifier

Klystrons, the most efficient of the linear beam tubes, are capable of the highest peak and average powers, and can be used over an extremely broad frequency range, from low ultra-high frequency (UHF) (200 MHz) to W-band (100 GHz) [14]. Klystrons make use of the transit-time effect by varying the velocity of an electron beam. Klystrons essentially consist of a series combination of high-Q cavities through which an electron beam passes, exchanging energy with an RF wave inserted into the input cavity. The RF is coupled from cavity to cavity via the electron beam itself, until it is amplified and extracted in the output cavity as shown schematically in Figure 2.21 below.

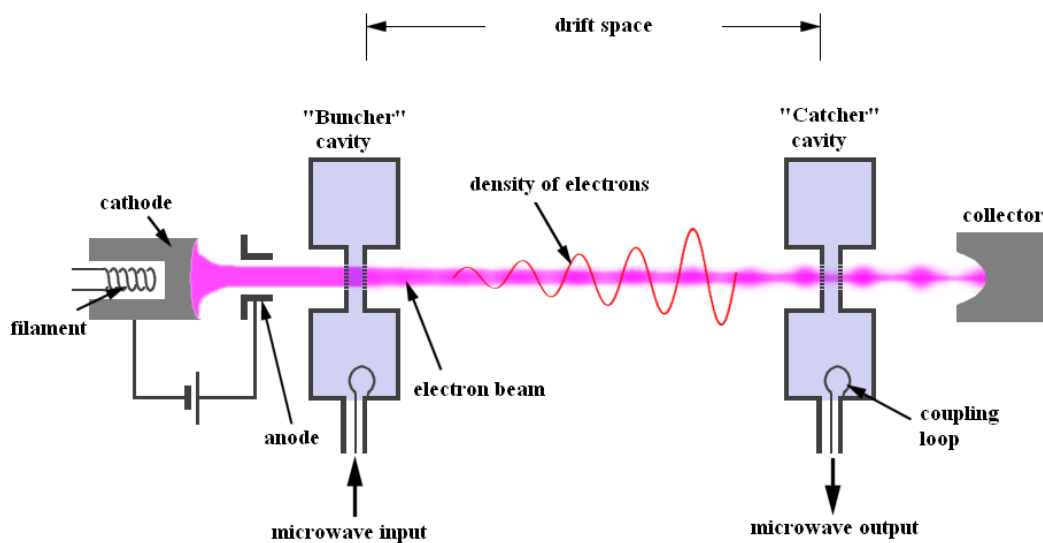


Figure 2.21. Schematic view of two-cavity klystron tube

Each cavity is a resonant circuit at a particular frequency. Tuning the cavities in different ways changes the overall characteristics of the amplifier. A given design can be tuned to give broader bandwidth at reduced gain or higher gain at reduced bandwidth. The

centre frequency can be changed by mechanically adjusting the cavity characteristics via the tuning adjustment.

The fact that the klystron uses high-Q cavities results in very low additive phase noise in the amplifier. Klystrons tend to have significant gain (40–60 dB) and good efficiency (40–60%) but suffer from inherently narrow bandwidth capability (about 1–10%) when compared with other tube types. Hence, for applications requiring a high power source with low phase noise but not much bandwidth, klystron is usually the proper choice.

Travelling Wave Tubes (TWT)

Like the klystron, the traveling-wave tube is a linear beam device. TWT are wideband amplifiers. They take therefore a special position under the velocity-modulated tubes [14]. On reason of the special low-noise characteristic often they are in use as an active RF amplifier element in receivers additional. There are two different groups on the basis of circuits used in TWT:

- **Low-power TWT**

The approach is helix and well suited for broadband operations. It occurs as a highly sensitive, low-noise and wideband amplifier in radar equipment

- **High-power TWT**

The approach is coupled cavity and used as a pre-amplifier for high-power transmitters.

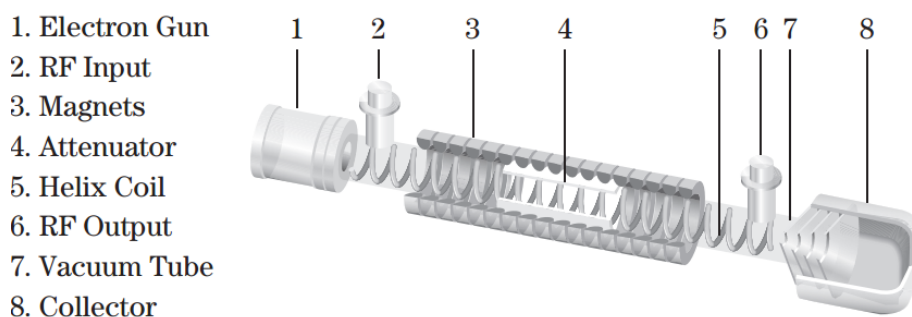


Figure 2.22. Functional diagram of TWT

Above Figure 2.22 is a functional diagram of a TWT showing its major components. An electron gun (1) emits a beam of electrons that passes through a slow-wave structure such as a helix (5) or coupled cavity. RF energy is injected into the tube via an input port (2) and removed via an output port (6). The velocity of the electron beam is set by the cathode-to-body voltage. The slow-wave circuit slows up the longitudinal component of the velocity of the RF signal so that it travels roughly in synchronism with the electron beam. Magnets (3) are used to keep the electron beam focused as it travels down the tube. As the beam and the signal traverse the length of the tube (7), the interaction causes velocity modulation and bunching of the electrons. The bunched beam causes induced currents to flow on the RF circuit, which then causes further bunching of the electron beam. Through this regenerative process, energy is transferred from the beam to the RF signal, and amplification of the RF signal occurs. The electron beam then strikes the collector (8), which dissipates the thermal energy contained in the beam. To reduce the impedance mismatches that will occur at the RF ports, and to decrease the backward wave that can flow in the tube, it is common to use an attenuator (4) to reduce these effects.

2.3.2. Receiver

The function of the radar receiver is to detect desired echo signals in the presence of noise, interference, or clutter. It extract information from the received echo by processing it, separate wanted from unwanted signals, and amplify the wanted signals to a level where target information can be displayed to an operator or used in an automatic data processor. The design of the radar receiver will depend not only on the type of waveform to be detected, but on the nature of the noise, interference, and clutter echoes with which the desired echo signals must compete. The two most important facts, which are very important for the radar receiver, are noise and clutter echo. Noise (internal and external) is the chief factor which limits the sensitivity of the receiver and clutter echo must be recognized to detect the desired target.

2.3.2.1. Super-heterodyne Receiver

The Figure below shows major components of the modern radar receiver. The principle, on which all radar receivers operate, is super-heterodyne [15]. The super-heterodyne receiver changes the RF frequency into an easier to process lower IF-frequency. Through this architecture, the receiver filters the signal to separate desired target signals from unwanted interference. After modest RF amplification, the signal is shifted to an intermediate frequency (IF) by mixing with a local-oscillator (LO) frequency. More than one conversion stage may be necessary to reach the final IF without encountering serious image- or spurious-frequency problems in the mixing process. The super-heterodyne receiver varies the LO frequency to meet any desired tuning variation of the transmitter without disturbing the filtering at IF. This simplifies the filtering operation as the signals occupy a wider percentage bandwidth at the IF frequency, which adds flexibility constrain in receiver.

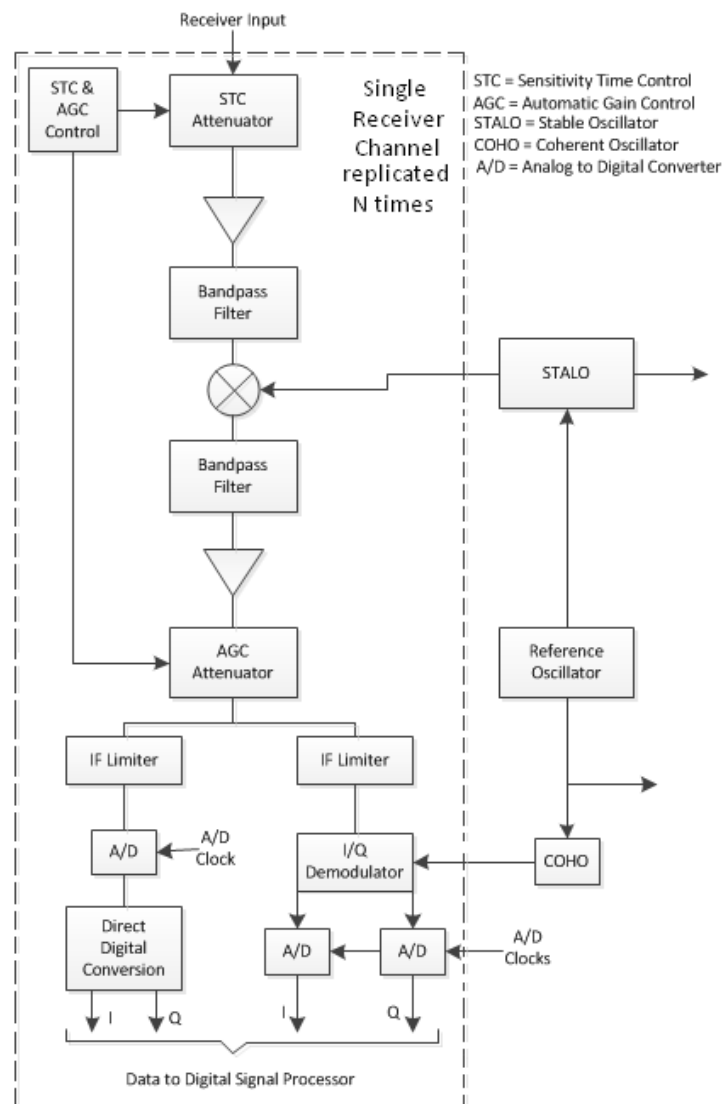


Figure 2.23. General Configuration of radar receiver

The block diagram shown in the above Figure includes sensitivity time control (STC) attenuator at the RF input. Alternatively adjustable RF attenuation may be used. Either form provides increased dynamic range above that provided by the analog-to-digital (A/D) converters. The STC attenuator is followed by an RF amplifier often referred to as a low-noise amplifier (LNA). This amplifier provides sufficient gain with a low noise figure to minimize the subsequent degradation of the overall radar noise figure by subsequent components. If sufficient gain is provided in the antenna prior to the receiver, it may be possible to eliminate this gain stage. The RF filter provides rejection of out-of-band interference, including rejection at the RF image frequency. After down-conversion to IF, a bandpass filter provides rejection of unwanted signals and sets the receiver analog-processing bandwidth. Additional gain is provided at IF to overcome losses and raise the signal level required for subsequent processing and to set the correct signal level into the A/D converters. An IF limiter limits large signals gracefully that would otherwise overload the A/D converters.

The two dominant methods of digitization, IF sampling and analog I/Q demodulation with baseband A/D conversion, are included for illustration in Figure, though in general, receivers will not include both techniques. Prior to the availability of affordable digital signal processing, a number of functions, such as monopulse comparison, currently performed in the digital domain, were performed using analog processing within the receiver.

All but the simplest of radars require more than one receiver channel. Figure shows a single receiver channel that may be replicated any number of times depending on the radar system requirements. Monopulse radars typically include three receiver channels, sum, delta azimuth, and delta elevation channels, used to provide improved angle accuracy. Additionally, many military radar systems include a sidelobe blanker or several sidelobe canceler channels to combat jamming. Since the advent of digital beamforming radar systems, the number of receiver channels required has increased dramatically, with some systems now requiring hundreds of receiver channels. In these multichannel receiver systems, close matching and tracking of gain and phase is required.

The stable local oscillator (STALO) block provides the local oscillator frequencies for downconversion in the receiver and upconversion in the exciter. For true coherent operation,

the STALO is locked to a low frequency reference, shown by the reference oscillator in Figure 6.1 that is used as the basis for all clocks and oscillators such as the coherent local oscillator (COHO) within the receiver and exciter. The clock generator provides clocks to the A/D converters and the direct digital synthesizer and provides the basis for the signals that define the radar transmit and receive intervals.

Almost all modern radar systems use digital signal processing to perform a variety of functions, including pulse compression and the discrimination of desired targets from interference on the basis of velocity or the change in phase from one pulse to the next. Previously, pulse compression was performed using analog processing with dispersive delay lines, typically surface acoustic-wave (SAW) devices. Analog pulse compression has largely been replaced by pulse compression using digital signal processing.

2.4. Some Limitations

We have seen in above discussion that in case of coherent radar the information is extracted from the change in the phase of the signal. So, in order to get good performance phase stability requires. It can be seen that there is mixing or frequency multiplication process involve in radar system both in case of up-conversion and down-conversion. This mixing process is actually a main source of phase noise in radar; it adds the frequency fluctuations and hence leads to errors. So, 1st thing we need is to get rid of this block. The other limitation is the processing speed of electronics which ultimately affects the performance of modern system. In radar receiver ADC involves, but electronic ADCs are limited in sampling rate and resolution (detail is in next chapter) which limits the realization of fast system.

3. Photonic based Radar: Characterization of 1x4 Mach- Zehnder Demux

In this chapter the scheme that has been used to implement the optical transceiver for a photonic assisted fully-digital radar system, based on optic miniaturized optical devices both for the optical generation of the radio frequency (RF) signal and for the optical sampling of the received RF signal, will be discussed. The focus will be mostly on the receiver side, especially on demux which is a critical block of the receiver. The architecture of optical radar is under experimental phase. The scheme for the generation of RF signal has been implemented with desired results and now experiments on receiver are being carrying out.

3.1. Overall Scenario

There are two main portion of the transceiver used to implement fully digital optical radar, one portion is to generate the radio frequency (RF) for radar by exploiting photonic. The other portion is the receiver side in which sampling of the received RF radar signal will be performed in photonic and then these samples will be further processed to get the required information. The proceeding discussion will be on these two portions.

3.1.1. Radio Frequency (RF) generation

In last chapter it is mentioned that coherent radar extract information from the phase of the echoes, so it can be concluded that for coherent processing of radar phase noise should be reduced as much as possible for better detection. Phase stability can be attained if we can remove the up-conversion in the transmitter. Photonic solutions have been proposed recently to avoid up-conversion in RF generation but these solutions don't provide a very stable RF generation [16]. In order to improve RF stability, phase locking is necessary. A relatively simple technique for generating phase locked laser lines is the mode locking of lasers: the intrinsic phase-locking condition of the mode-locked laser (MLL) ensures an extremely low phase noise of the generated RF signal. So, MLL can be used to improve the performance of radar transmitter.

For radar transmitter the technique proposed in [16] is based on MLL, same sampling MLL of receiver, and exploiting phase stability of it. The basic idea for generating a stable radar signal is reported in below Figure 3.1.

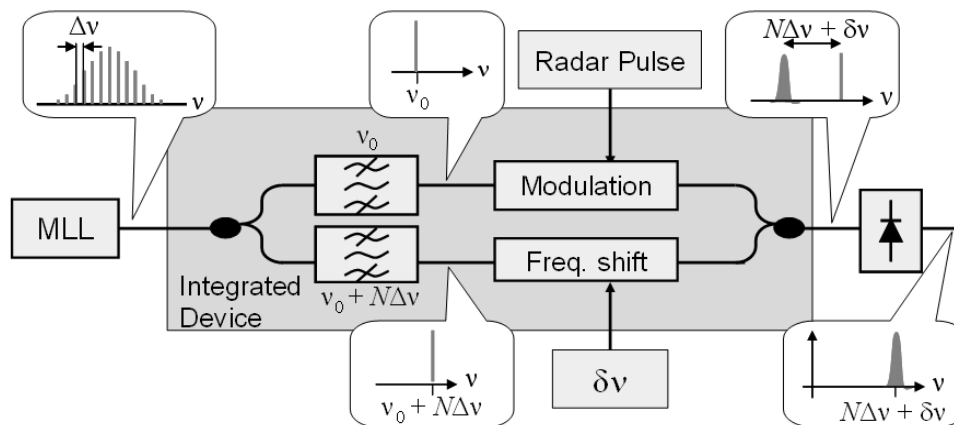


Figure 3.1. Basic scheme for the generation of radar signal using same MLL used in optical-sampling of receiver

The signal from MLL is split into two separate paths, where two different modes are selected at v_0 and $N\Delta v$ with the help of filters. One mode on one path is modulated to shape the radar pulse while the other mode on second path is frequency shifted. Frequency shift is required to get RF signal at required high frequency as we are using one MLL for transmitter and receiver at sampling rate. The two processed modes are then combined and detected in photodiode. This will generate the beating at the frequency $(N\Delta v + \delta v)$ or $(N\Delta v - \delta v)$, depending on the sign of frequency shift. There will be negligible increase of phase noise

w.r.t original MLL. The variant of this technique has also been proposed in which two modes are filtered before splitting as shown below in Figure 3.2.

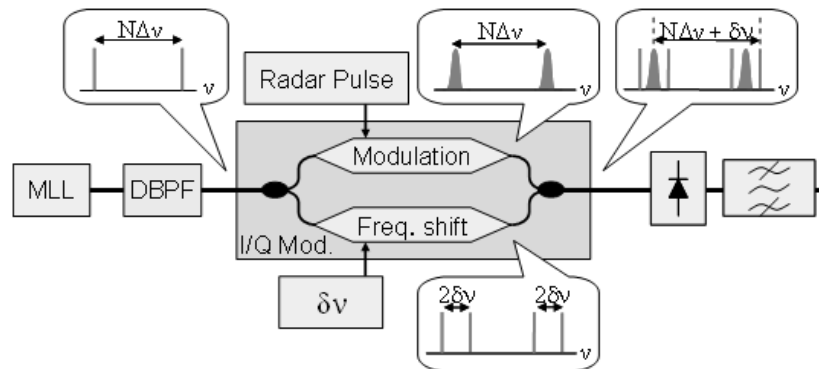


Figure 3.2. Advance scheme exploiting optical I/Q modulator

The benefit of this technique is that in this way we can use commercial available I/Q modulator but in previous case we need custom built-in integrated photonic device to avoid phase fluctuations. I/Q modulator can provide frequency shift as well as RF pulse modulation as shown in above figure. DBPF (Double band-pass filter) should be used to select two modes from MLL, an example of DBPF is Fabry-Perot filter followed by a suitable band-pass filter. The two selected modes will be simultaneously sent to both arms of modulator. On one arm the two modes are modulated by radar pulse while on the other arm a carrier-suppressed modulation driven by low frequency oscillator splits the two modes into new spectral components at $\pm \delta v$ from the original modes. The processed signals from two arms are combined and detected by photodiode where the beating of all these frequency components occurs. A microwave filter can then filter out the desired signal produced by beating.

In this case it will be easier to use tuneable filters; the only cost to pay in this technique is the need for a microwave filter after photodiode, since it will filter the signal at required frequency from the beating of frequency components at $N\Delta v$, $(N\Delta v \pm \delta v)$ and $(N\Delta v \pm 2\delta v)$.

Experimental results

MLL at 9.953GHz has been used. Two adjacent modes ($N = 1$) are filtered and sent them to I/Q modulator. A sine modulation at 47MHz is used for frequency shifting both the

lines. The RF pulse is a squared pulse, $1\mu\text{s}$ pulse width over $3\mu\text{s}$ period. A RF filter at 10.0GHz is used to select the shifted signal. We first avoid the RF modulation to study the carrier stability as shown in below Figures 3.3.

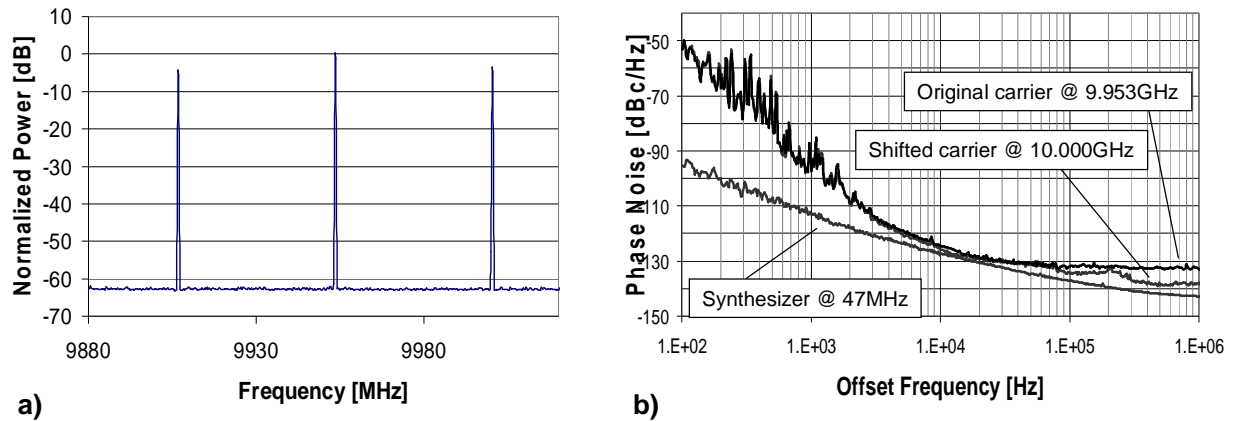


Figure 3.3.a) Electrical spectrum after the photo-diode, radar pulse modulation is off, b) Phase noise measure of the shifted carrier, compared with the original carrier and with 47MHz synthesizer.

Figure 3.3 a) above shows the electrical spectrum of the signal after the photodiode when the radar pulse modulation is off and the shifting sinusoidal is on. Two shifted carriers are generated around the original one at 9.953GHz . The figure demonstrates the generation of a highly pure sinusoidal carrier, showing a side mode suppression of the carrier at 10GHz greater than 50 dB . The phase noise of the shifted carrier is studied in next Figure 3.3 b), where it is compared with the phase noise original MLL and of the 47MHz synthesizer. The synthesizer shows a phase noise much lower than the original MLL; therefore the 10GHz carrier shows a phase noise curve that largely follows original MLL. The two curves coincide for the offset frequencies up to 100 kHz , while the shifted carrier shows the noise floor 5 dB higher for higher frequency offset. Integrating the phase noise from 1 kHz to 1 MHz , which is the frequency range of interest for radar application, an RMS jitter of 12 fs and 12.4 fs is calculated for the original MLL and for the shifted carrier respectively. The remarkable small difference in time jitter confirms that the frequency shift operation does not introduce significant phase noise, allowing the generation of an ultra- stable RF carrier.

When applying the radar pulse modulation, the shifted carrier is modulated too and the desire RF signal is produced. In Figure 3.4 a) the spectrum of the base-band radar pulse is shown; the inset also reports the time trace of the rectangular radar pulse. Next Figure b)

shows the beating generated by the photodiode when the radar pulse modulation is active; the three carriers shown are all modulated. In last Figure c) the spectrum of signal of interest at 10GHz after the microwave filter is reported. The modulation spectrum correctly moved around the shifted carrier, although the effect of microwave filter is visible. The inset also shows the time trace at the oscilloscope as expected, the signal shows the envelope of the radar pulse modulated by the carrier at 10GHz.

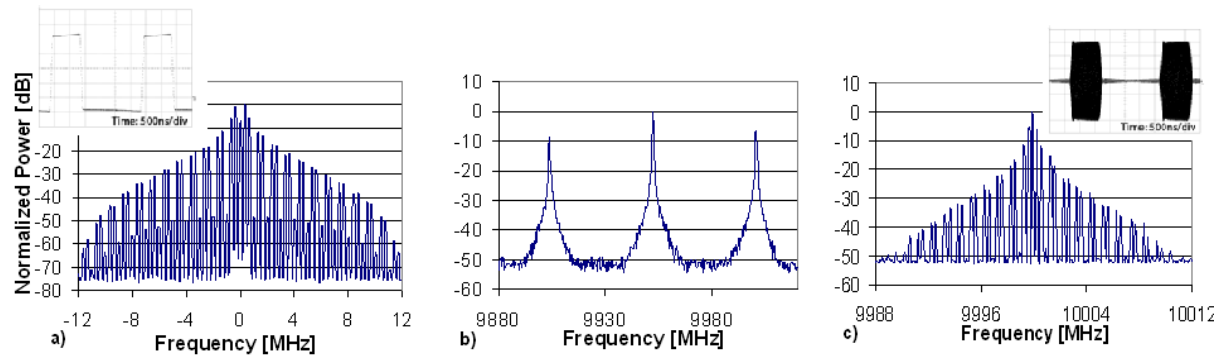


Figure 3.4. a) Base-band spectrum (RBW=30kHz) and waveform (inset) of the radar pulse. b) Spectrum (RBW=300kHz) of modulated carriers, after the photodiode. c) Spectrum (RBW=30kHz) and waveform (inset) of filtered radar signal.

In [17] a phase modulated RF signal generation with pulse compression technique in coherent radar has been reported to increase the resolution of radar. Pulse compression is demonstrated by utilizing Barker code.

3.1.2. Radar Receiver

As discussed in RF signal generation about up-conversion as source of phase noise, similarly current electronic receiver for coherent radar use down-conversion by mixing the received signal with local oscillator. This mixing process leads to phase instability, so we need a technique to avoid down-conversion as well. By using photonic assisted analog-to-digital converter technique we can avoid this down-conversion process. The received signal is directly converted to digital form then analysed. Moreover currently available electronics ADCs are limited in resolution (Effective Number of Bits (ENOB)) and sampling rate which can be tackled very efficiently in photonic ADCs.

The rate-of-improvement of high-speed electrical ADCs is substantially slower than that of digital signal-processing (DSP) hardware. The electronic ADCs are not able to fulfil the requirements of high resolution which is needed in modern systems like radar. The

resolution of electronic ADCs is limited, in addition to the inherent quantization noise, by a number of mechanisms including thermal noise, sampling aperture jitter, and comparator ambiguity [2]. The equations [2] that calculate the associated maximum achievable resolutions, in SNR-bits, are

thermal noise (referred to the input):

$$B_{\text{thermal}} = \log_2 (V_{\text{FS}}^2 / 6kTR_{\text{eff}}f_{\text{samp}})^{1/2} - 1$$

where, V_{FS} = Full scale voltage, R_{eff} = Thermal noise resistance, k = Boltzmann's constant (1.380658×10^{-23} J/K) and T = temperature in Kelvin

aperture uncertainty:

$$B_{\text{aperture}} = \log_2 (2 / \sqrt{3\pi f_{\text{samp}}\tau_a}) - 1$$

Or

$$\text{ENOB} = \log_2 (2 / \sqrt{3\pi f_{\text{samp}}\tau_a})$$

where, τ_a = RMS aperture jitter (standard deviation of the variation of the sampling point, sampling jitter)

comparator ambiguity:

$$B_{\text{ambiguity}} = (\pi f\Gamma / 6.93f_{\text{samp}}) - 1.1$$

where, $B_{\text{ambiguity}}$ reflects the probability that the comparator will make an ambiguous decision

From above expressions SNR curves, shown in the below Figure 3.5, are calculated in [2] for values of thermal noise, aperture jitter, and $f\Gamma$ which measures comparator ambiguity. Assume $V_{\text{FS}} = 1\text{V}$, $T = 300\text{K}$ for the thermal noise curves. Aperture jitter is calculated for Nyquist sampling, i.e. $f_{\text{sig}} = f_{\text{samp}} / 2$. Comparator ambiguity is determined from the regeneration time constant of the IC technology.

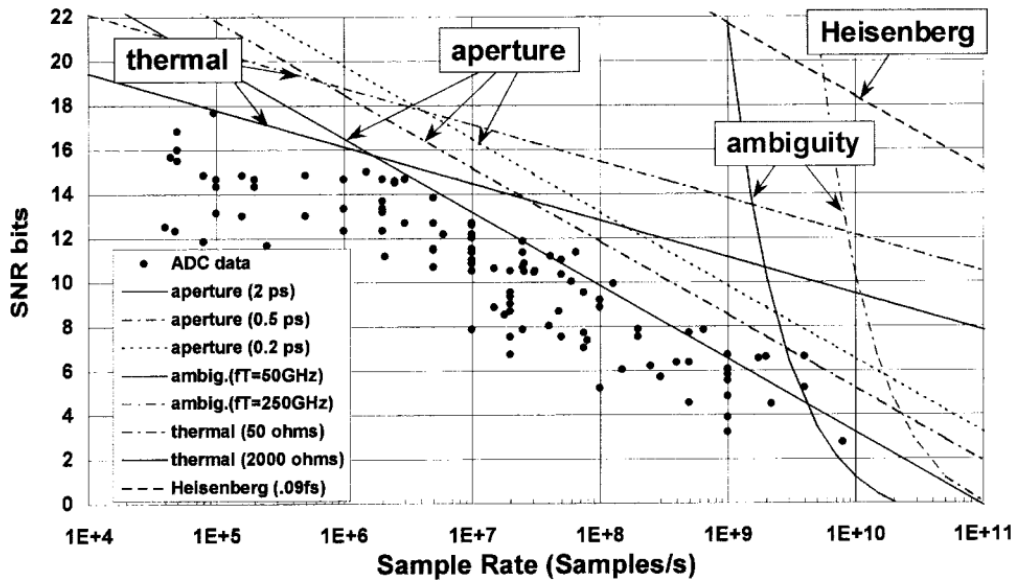


Figure 3.5. Survey ADCs

It can be observed from above curves that thermal noise appears to dominate the performance of high-resolution low-bandwidth ADCs while aperture jitter and comparator ambiguity become important at high sampling rates. The current state-of-the-art is limited by the equivalent of thermal noise associated with a $\sim 2 \text{ k}\Omega$ resistor for sampling rates under 2 Ms/s. Aperture jitter, in the range 0.5 ps to 2 ps, limits SNR for the sampling frequency range of $\sim 2 \text{ Ms/s}$ to 4 Gs/s. Comparator ambiguity is limited via the regeneration time constant corresponding to a value of $fT \sim 50 \text{ GHz}$ for ADC's at the highest sampling rates. So, it can be concluded that in order to attain high resolution high sample rate ADCs, aperture jitter and comparator ambiguity has to be reduced.

Let's assume that jitter is the only error source, Figure 3.6 below shows the allowable timing jitter for a Nyquist ADC (i.e., maximum input frequency ($f_{\text{sig}} = 1/2$ sampling rate (f_{samp})) as a function of sampling rate and effective bits [18]. Estimates of aperture jitter in state-of-the-art electronic ADCs range from 0.5 to 2 ps (see hatched region in below Figure), indicating that electronic aperture jitter is presently a major limit to the performance of high-speed high-resolution ADCs [18]. For example, the 50-fs timing jitter required to implement a 1- GS/s 12-bit converter is far below that of present electronic jitter estimates. In contrast, sampling-aperture jitter less than 50 fs has been attained in optical sampling systems.

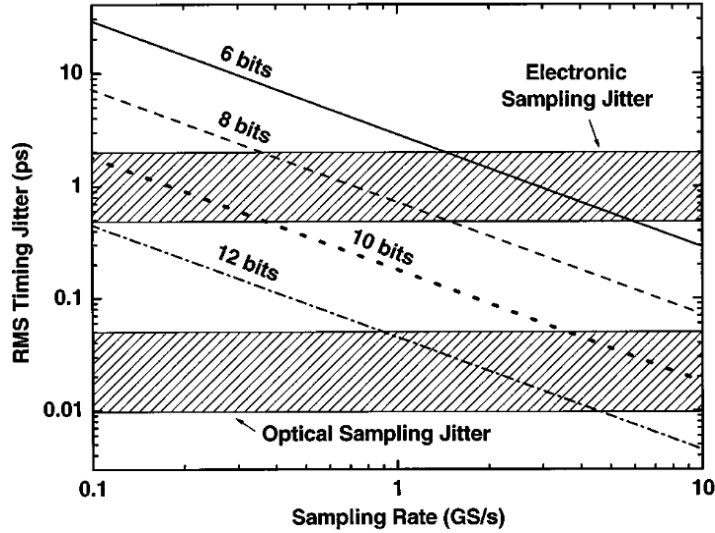


Figure 3.6. Timing-jitter requirement for ADCs as a function of sampling rate and number of effective bits. The calculation assumes that timing jitter is the only noise source.

From the developed arguments given in above paragraphs it can be concluded that 1st of all we needed a technique to attain very low (fs) timing jitter which will result in high resolution ADC. A very attractive solution to get low timing jitter is to sample the signal in Photonic domain using mode-locked laser. The principal advantages of optical sampling are: 1) modern mode-locked lasers can produce high-frequency (10 GHz) periodic sequences of optical pulses with timing jitter significantly below that of electronic circuitry, and 2) the sampling process can be made to be highly linear with negligible back-coupling between the optical sampling pulses and the electrical signal being sampled. The timing jitter of actively mode-locked fiber lasers has been measured to be 10 fs over narrow-band integration limits (100 Hz to 1 MHz) and 50 fs pulse to pulse (see hatched region in Figure 3.6).

In our radar receiver we are sampling the received radar signal in photonic domain to get the benefit of low timing jitter in sampling and then utilizing well developed electronics technology for quantization to minimize the cost as well. Our aim is to get ENOB value of 10bits.

3.1.2.1. Photonic Sampled and electronically Quantized ADCs

Mode-locked laser can be used to sample an RF signal was discussed first by H. F. Taylor, M. J. Taylor, and P. W. Bauer in Applied Physics Letter (1978) as part of their all-optical ADC. Later, Bell *et al.* (1989) recognized that optical sampling and temporal demultiplexing would be useful for making a time-interleaved ADC. In 1989 1st they had

analysed and indicated that precision of 6 bits should be attainable by a system which includes an actively mode-locked diode laser operating at 4 GHz (4GS/s), and a 1x8 time demultiplexer. Then in 1991 they had demonstrated a system which uses 4 parallel electronic A/D converters and a pulsed diode laser with a sample rate of 2 GHz. The precision of this system is as high as 2.8 effective bits. After that, many researchers (1992 - 2004) have concentrated on the optical sampling process alone without demultiplexing to take advantage of the short pulse widths and low pulse-to-pulse jitter of a mode-locked laser. The basic components of an optically sampled system consist of a stable pulsed laser, an optical modulator, and a detector/integrator [19] as shown in Figure 3.7 below.

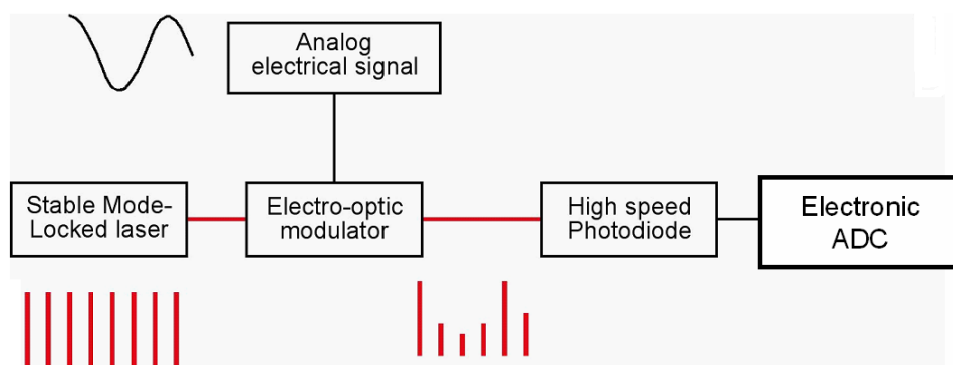


Figure 3.7. Photonic sampled and electronically quantized ADC.

In optically sampled ADCs, the optical pulse generator is typically a mode-locked fiber or semiconductor laser, the optical modulator is typically a LiNbO₃ Mach-Zehnder modulator, and the detector is a high-speed photodiode. This system contains an analog optical link and thus its performance is characterized by the link SNR, SFDR, modulator bandwidth and modulation index, photodiode saturation current and bandwidth [19].

The technique to implement ADC for our radar receiver is based on the very impressive work done in [18] to attain resolution of 10bits with fast sampling rate. The block diagram of the scheme is given in below Figure 3.8:

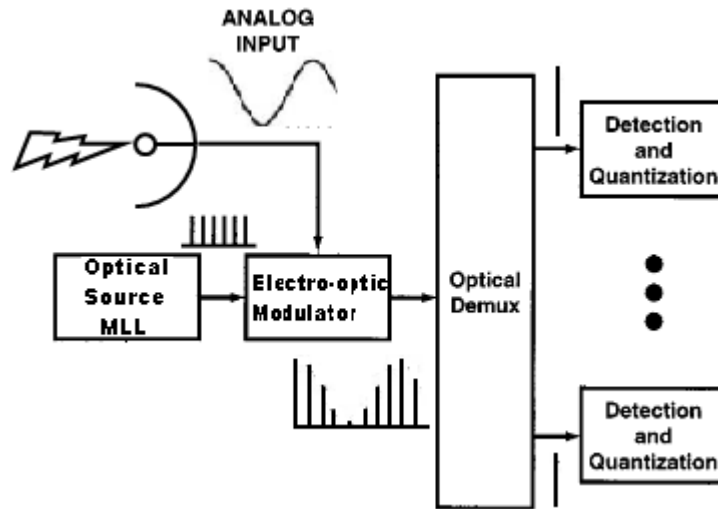


Figure 3.8. Generic architecture of an optically sampled time-interleaved ADC

There are three main components in the above mentioned scheme:

1. Mode Locked Laser (MLL): to get low jitter train of pulses at required rate for sampling.
2. Electro-optic Modulator: to sample received radar signal with precisely timed optical pulses from MLL that converts electrical signal variations into optical-pulse intensity or energy variations.
3. Optical Demux (OTDM): to parallelize the post-sampled pulses so as to meet the processing speed of electronic ADC used for quantization. In short demux is used to rate reduced the sampled pulses.

Figure 3.9 shows different components used in receiver. To implement the photonic sampling process MLL having repetition rate of 400MHz with 1ps pulse width has been used to generate 400MS/s. The received RF radar signal at 9900MHz will be sampled by using LiNbO₃ Mach Zehnder Modulator (MZM). This MZM will convert the electrical signal variations into amplitude-modulated optical pulses at the rate corresponding to MLL. Then optical 1x4 demux, clocked at 200MHz and 100MHz, used to parallelize the post sampled pulses to rate reduce the sampling rate at 100MHz to meet electronic speed of ADC. The further detail about optical demux will be given later. One thing which is worth mentioning is the use of Dispersion Compensation Fibre (DCF) before photodiode. The optical peak power limits the power at the photodiodes, and hence the amplitude of the signal at the ADC. The DCF is used to broaden the pulse and hence increase the efficiency.

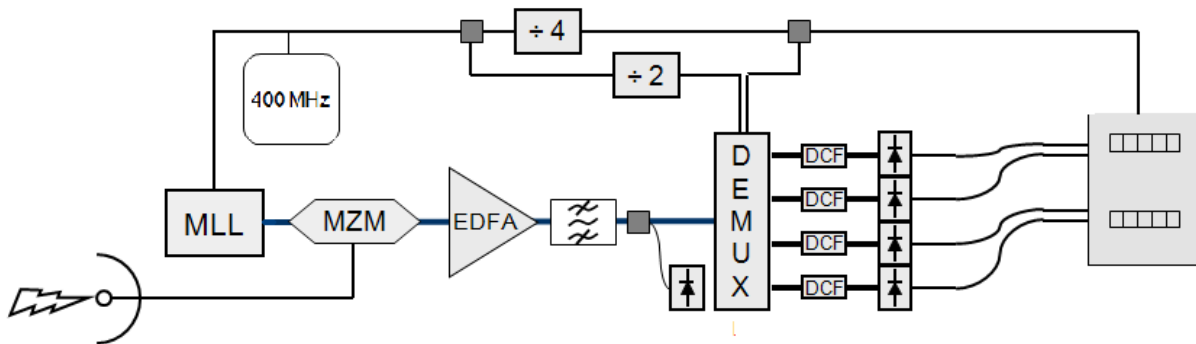


Figure 3.9.Components of radar receiver scheme

3.2. Characterization of 1x4 Mach-Zehnder Demultiplexer (demux)

Optical demux is a very critical block of the receiver used for the parallelization of the optical samples, by employing optical time division demultiplexing, and it strongly impacts the performance of the whole system. While the linearity and dynamic range of an A/D converter can be enhanced by employing optical sampling, the sampling rate is limited by the speed with which the associated electronic A/D converter can quantize the detected optical pulses. An attractive means for increasing the sampling rate and on the same time to meet electronic processing speed is to use a 1: M demux at the output of the electro-optic modulator to direct sequential optical pulses to a parallel array of electrical A/D converters each operating at a quantization rate of f_{samp}/M where f_{samp} is the aggregate sampling rate. We are using time-division demultiplexing technique to parallelize the samples. The input pulses are all at the same wavelength i-e at 1550nm. The demux consists of an array of electrically driven optical switches (e.g., a cascade of 1 x 2 electro-optic switches) that direct the sequential optical pulses to the appropriate detectors and electronic A/D converters.

In order to realize a demux we need a design which can fulfil all the system specifications. The solution should be compatible with the Mach Zehnder modulator (used for sampling) and the final photo-detector technology, enabling a higher level of compactness of the whole system. The frequencies of interest for this application are lower than few GHz for the sampling rate and hundreds of MHz for the parallel sampling flows, making the chosen technology an appropriate solution, able to guarantee low noise, low attenuation and

high sensitivity. Beside this, we also took into consideration the low cost factor, complexity and integration. A 1x4 demux has been developed using Mach Zehnder Interferometers, an electro-optic solution, as a switch matrix. Mach Zehnder can be precisely controlled to attain the stability and also provide high extinction ratio to minimize cross-talk between channels. Cross-talk adds spurs in the signal. Due to the integrated structure sufficient stability as well as balanced path to provide correct synchronism between optical and electrical control signals can be attained. So, a 1x2 Mach Zehnder switch has been used in two stages to get 1x4 demux as shown in below schematic.

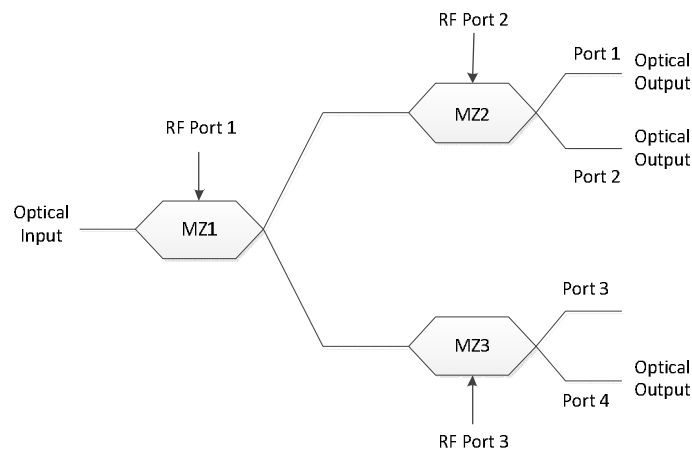


Figure 3.10.MZ switch matrix

3.2.1. Technological aspects

The MZM chip is realised in integrated optics on LiNbO₃, the optical waveguides are realised in Thermal Annealed Proton Exchange (TAPE) technologies that allows a higher optical power damage threshold with respect to Ti diffusion. The thin film electrodes are defined by deep UV photolithography, the microwire thermosonic bonding allows the electrical interconnection in the package and also the SM fiber pigtail is implemented. An example of packaged device is shown in Figure 3.11

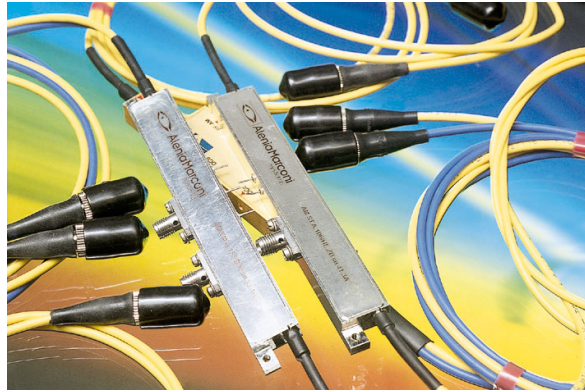


Figure 3.11. Packaged demux

The 3 MZM modulators allow the dual output modulation as shown in Figure. 3.12. The optical couplers are electro-optically tuned in order to achieve an optimum optical extinction ratio (E_r) of the MZM and to provide more control. To operate the MZM in any working point (and particularly for quadrature point), a bias voltage is needed on the RF electrode, and then the device should be equipped with bias-T circuit.

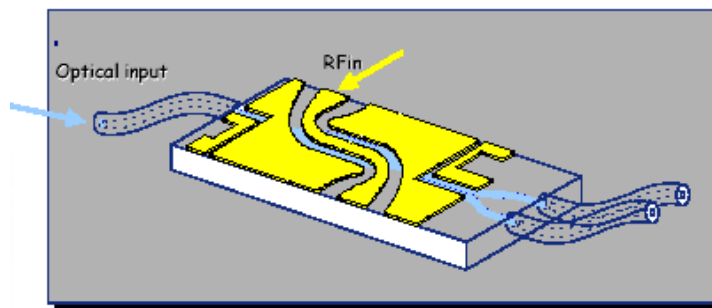


Figure 3.12. Internal structure of MZ

In order to reduce the rate of 400MHz post sampled pulses to 100MHz, we need a clock of 200MHz at the RF port of 1st stage of demux to obtain pulses at 200MHz. Then RF ports of the second stage will be provided with clock of 100MHz to get pulses at 100MHz. This clock will be provided by dividing the MLL output by 2 and 4 to get 200MHz and 100MHz pulses respectively. Figure 3.13 shows the signal definition before and after demux. There is a phase change of 90° after 1st stage.

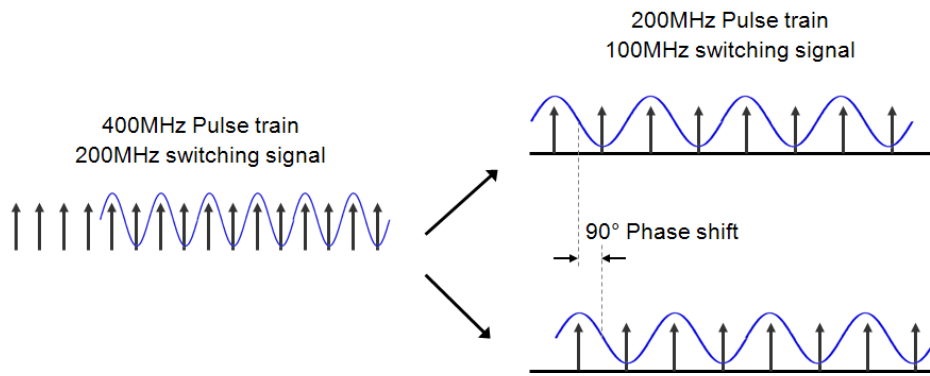


Figure 3.13. Signal definition before and after demux

For these RF signals we need to match the impedance and along this we need to develop bias-T to provide DC as well.

3.2.2. Mach Zehnder as Switch

Among different topologies, MZI structures are most efficient, converts a phase modulation into an intensity modulation, which is widely used for many optical applications e.g. modulators etc. Monolithically integrated MZI switches represent the most promising solution due to their compact size, thermal stability and low power operation. Basic 2x2 MZI switch structure can be viewed, as shown in Figure 3.14 below, as two interferometric arms of equal length connecting two couplers. The first coupler is used to split the signals in two beams, which when passed through the interferometric arms experiences phase difference. This phase difference is due to voltage variations across electrodes covering interferometric arms that in turn changes refractive indices. Finally, both the beam with different phases are put together again into a single signal by the second coupler, and the outputs are observed as per constructive or destructive interference.

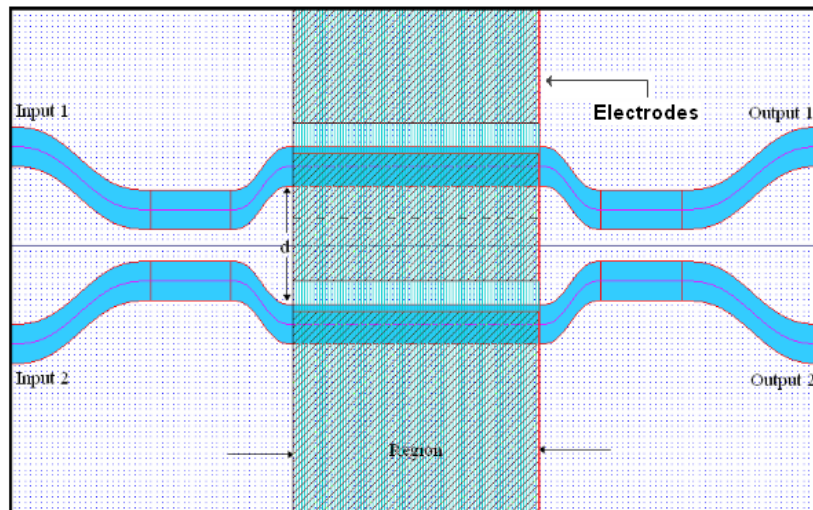


Figure 3.14.2x2 MZ switch layout

In our case we need a switch with one input so we have used MZI with one input close. The input signal will be split among two waveguides and then undergo the phase change due to applied voltage. When the signal will be combined in the coupler, an electro-optic, then there will be a destructive interference on one port and constructive interference on the other port to output the optical signal only from one of the outputs at one time.

3.2.3. Matching and Biasing network

Impedance matching is needed to provide maximum power transfer between the source or RF energy and its load. The first reason for matching is just power efficiency. The second reason is device protection. If RF circuit is not matched we get reflected power. This reflected power builds standing waves on the transmission line between the source and load. Depending on the phase between the forward and reflected both waves can either subtract or add. Because of that on the line we can get places where the voltage is the sum of either voltages or eventually places where the voltage equals zero (maximum current). For RF input, as in our case, the condition for impedance matching is that real part of the impedance should be equal to the real part of the load and reactance should be equal and opposite in character. For example if our source impedance is $R + jX$ to achieve matching our load should be $R - jX$.

Following are the demux specifications to match:

- Input reflection coefficient @ 100 MHz $S_{11} = 0.976 \exp(-j0.209)$ corresponding to load impedance of $z = 476.5 \exp(-j1.45)$ Ohms.
- Input reflection coefficient @ 200 MHz $S_{11} = 0.986 \exp(-j0.327)$ corresponding to load impedance of $z = 302.9 \exp(-j1.52)$ Ohms

All the impedances are matched against source resistance of 50 Ohms. The circuit diagram used to build the matching and biasing network is shown below along with the developed matching network.

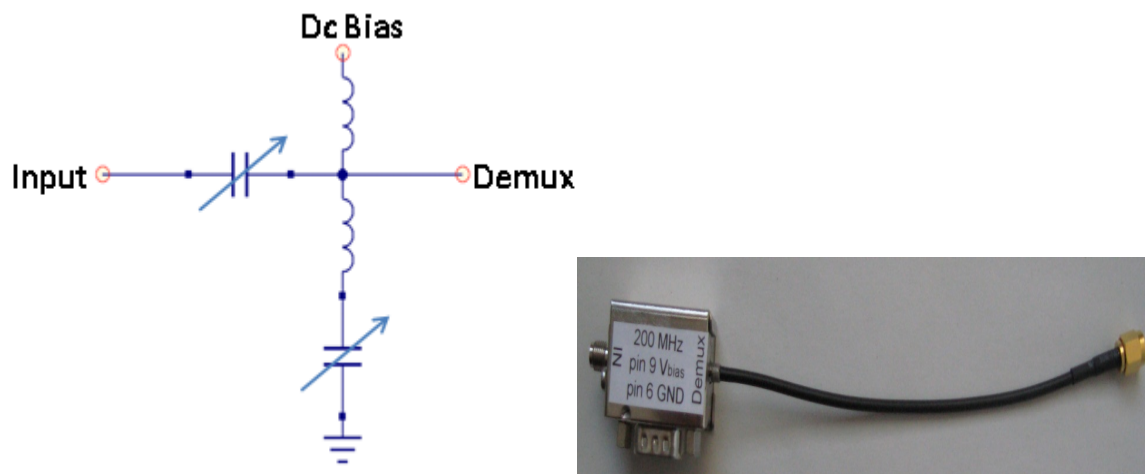


Figure 3.17. Matching and biasing network circuit diagram and packaged device

The magnitude of scattering parameter, at 200MHz and 100MHz, after impedance matching is shown below in two graphs. These graphs have been taken by mean of network analyzer. The dips in these graphs at 200MHz and 100MHz clearly depict low magnitude of scattering parameter which is the need of scheme.

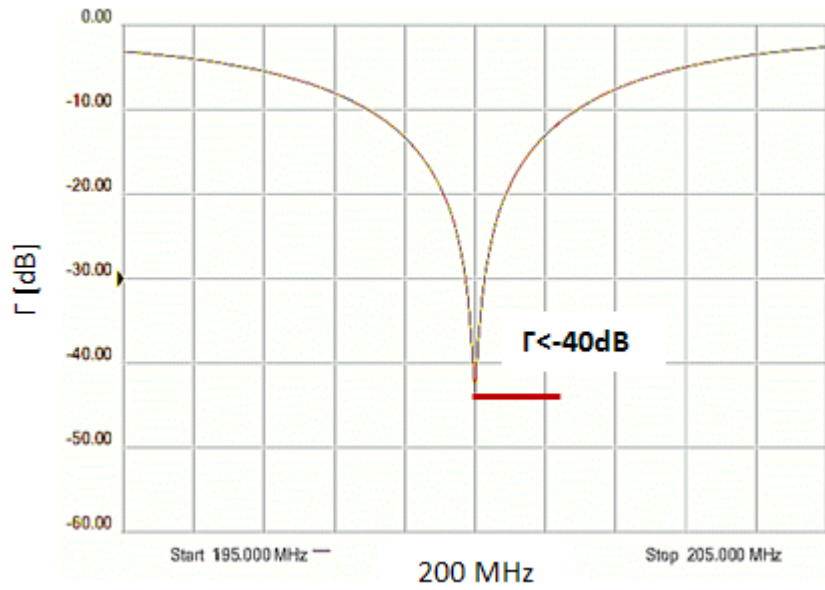


Figure 3.16. Magnitude of S11 parameter at 200MHz after impedance matching

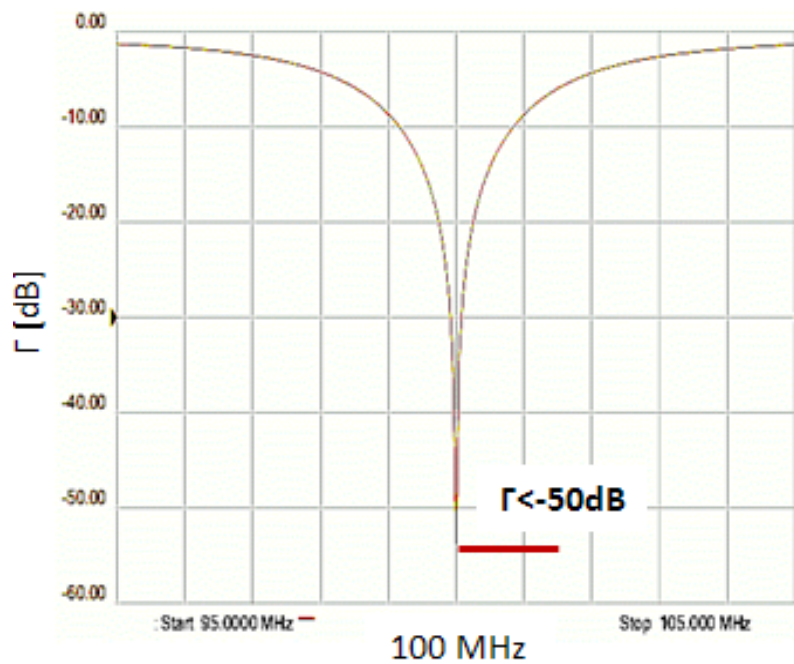


Figure 3.17. Magnitude of S11 parameter at 100MHz after impedance matching

After matching the impedance we need to find different voltage values to control demux and to get required results. As described above that optical signals from two MZ arms are coupled using electro-optic coupler. So, we need to find the voltages ($V_{\text{bias coup}}$) to control the coupler and to operate the coupler accordingly.

3.2.4. Coupler Bias Voltage ($V_{\text{bias coup}}$)

The electro-optic coupler is an important application of electro-optic effect use to control the optical devices. This can be used to transfer the light from one waveguide to the other, so that the device serves as an electrically controlled directional coupler. Two parameters govern the strength of this coupling process: the coupling coefficient C (which depends on the dimensions, wavelength, and refractive indices), and the mismatch of the propagation constants $\Delta\beta = \beta_1 - \beta_2 = 2\pi\Delta n/\lambda_0$, where Δn is the difference between the refractive indices of the waveguides. The coupling efficiency can be controlled by external voltage level applied through the electrode as shown in Figure 3.18. The applied voltage will determine the amount of optical power transmitted to a particular output port.

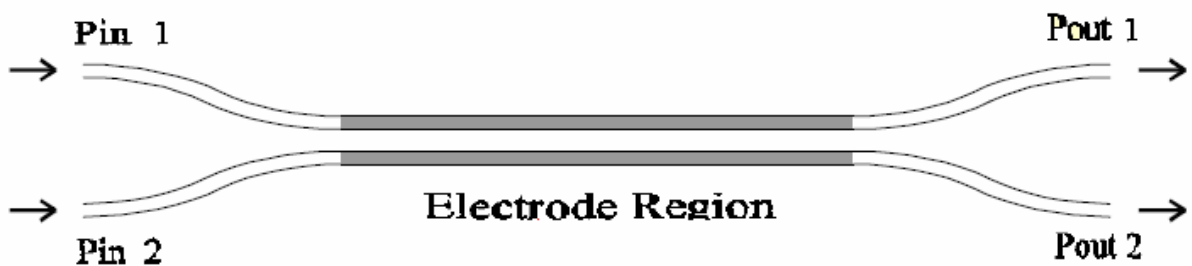


Figure 3.18. Schematic of electro-optic coupler

A dependence of the coupled power on the phase mismatch is the key to making electrically activated directional couplers. The power transfer ratio in phase mismatch case, $\beta_1 \neq \beta_2$, is $T = P_2(L_0)/P_1(0)$ which depends on phase mismatch parameter, $\Delta\beta L_0$ where, $L_0 = \pi/2C$. Here the ratio is based on one input $P_1(0)$ in one of the waveguide, same theory can be applied on other input also. Now the power transfer ratio is:

$$T = (\pi/2)^2 \text{sinc}^2 \{ 1/2[1 + (\Delta\beta L_0/\pi)^2]^{1/2} \}$$

The $\Delta\beta$ of the phase mismatch $\Delta\beta L_0$ can be controlled by mean of electro-optic effect. This leads to the dependency of T on applied voltage V and T becomes:

$$T = (\pi/2)^2 \text{sinc}^2 \{ 1/2[1 + 3(V_{\text{biascoup}}/V_s)^2]^{1/2} \}$$

where, V_s is switching voltage

Now what we need to find an operating voltage V_{biascoup} where the coupling will be 50/50 i-e T should be one half. This means that half power from any of the waveguide will remain in the same waveguide and half will transfer to the other waveguide. This implies for both of the input signals. In order to find coupling bias voltage, V_{biascoup} , we need to control bias Voltage of each MZ and then to measure the extinction ratio at the output ports of the demux. To find the V_{biascoup} following setup has been made:

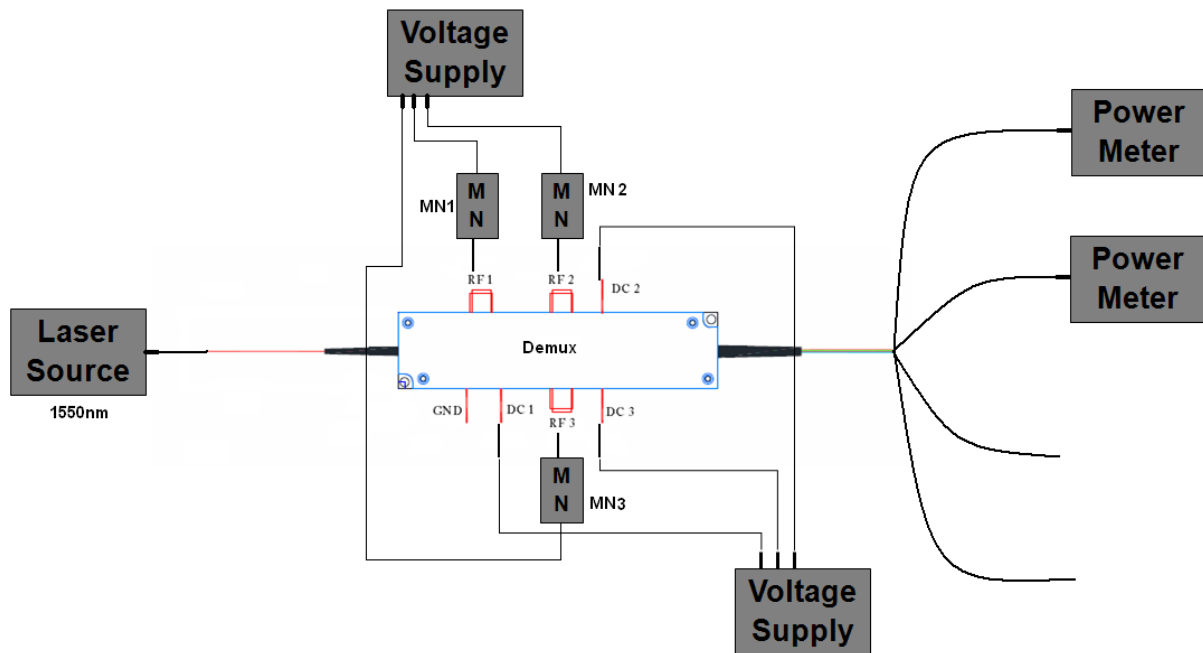


Figure 3.19. Experimental setup to find V_{biascoup}

The way to find V_{biascoup} was:

1. Consider one coupler at one time and apply different values of V_{biascoup} to that coupler e.g to coupler 3 at DC 3.
2. For each value of V_{biascoup} applied, vary the V_{bias} of respective MZ, e.g MZ3 in case of coupler3, and for each value of V_{bias} measure the output power from the respective ports, port 3 and 4 in case of MZ3. The voltages to all other couplers and MZ will be adjusted to get high output power.
3. Then Extinction Ratio (Er) has been measured at each V_{biascoup} point. After that all the results are compiled to find 50/50 coupling V_{biascoup} and Er at that voltage.

In order to measure the coupler bias a program has been made on *LabView* to provide different voltages by controlling the voltage supply and then reading the output power from power meters. The voltage supplies and power meters have been controlled through the program made in *LabView*. There is different sequence of coupler bias and MZ bias values that has to be provided to one MZ at one time. There are two loops that are controlling the voltage supplier. The outer loop provide different values of V_{biascoup} and for each value of outer loop the inner loop will provide V_{bias} to the MZ which is under observation, provided all the other coupler and MZ biases are adjusted at the values where output power is maximum. The next step is to measure the output power from demux ports. This has been done by controlling two power meters by mean of *LabView*. In this case we were able to find E_r of output optical signal from different ports and then to find the operating point of couplers.

A number of experiments have been carried out in the Lab with above mentioned setup and then results have been collected and observed. Due to the effect of temperature on MZ the experiments have been carried out on different temperature values. The temperature of MZ has been controlled by temperature stabilizer. Below is the description of the experiment results that has been taken.

Temperature 27 °C

Below is the graph, Figure 3.20, that is showing the E_r of output optical signals versus V_{biascoup} at 27 °C temperature for MZ1 (at stage one of demux). The output has been collected from port2 (one output port from MZ2) and port3 (one output port from MZ3) and the coupler and MZ bias voltages have been provided on DC1 and MN1 (follow Figure 3.18 for better understanding) respectively.

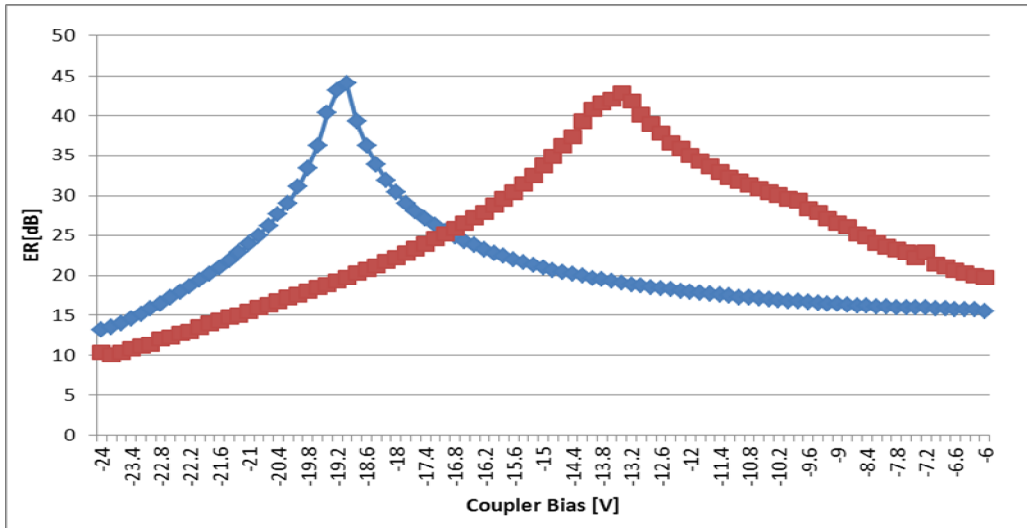


Figure 3.20. Coupler bias vs Output Er for coupler1 of MZ1 at temp. 27

By observing the above output graph the coupler bias voltage of 1st coupler for 50/50 coupling comes out to be -17 V at extinction ratio of almost 25 dB.

For coupler2 $V_{bias\,coup}$ has been provided at DC1 port and MZ2 bias on MN2. The output power has been measured from port3 and port4. The bias voltages of other couplers and MZs have been set on the fixed voltages. The graph for coupler2 is shown below, Figure 3.21. The graph shows that 50/50 coupling voltage is at -22 V and extinction ratio of output optical signal from two ports at that voltage is almost 23 dB.

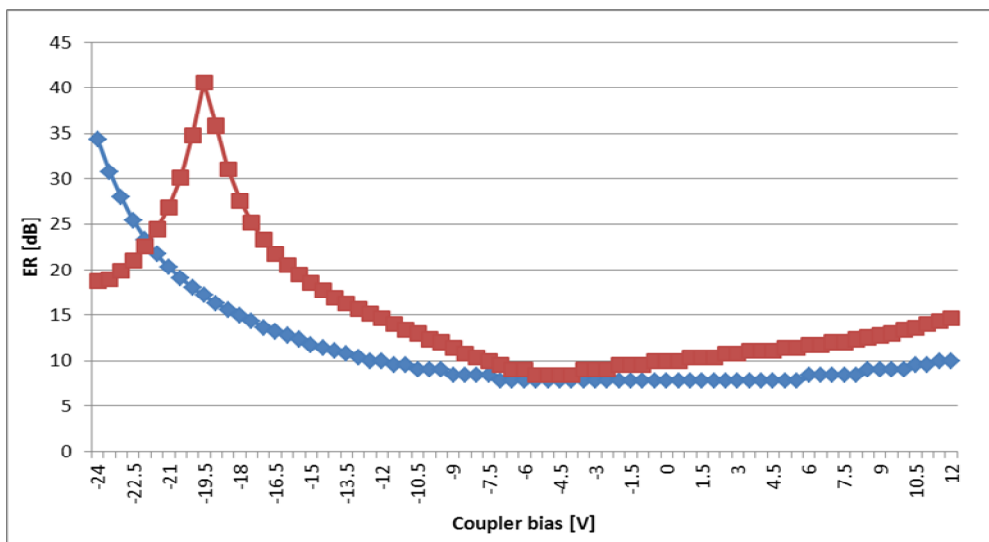


Figure 3.21. Coupler bias vs Output Er for coupler2 of MZ2 at temp. 27

Now for the last coupler i-e coupler3, $V_{\text{bias,coup}}$ has been provided at DC3 port and MZ3 bias on MN2. The output power has been measured from port1 and port2. The bias voltages of other couplers and MZs have been set on the fixed voltages. The graph for coupler3 is shown below. The graph shows that 50/50 coupling voltage is at -22.6 V and extinction ratio of output optical signal from two ports, at that voltage, is almost 23 dB.

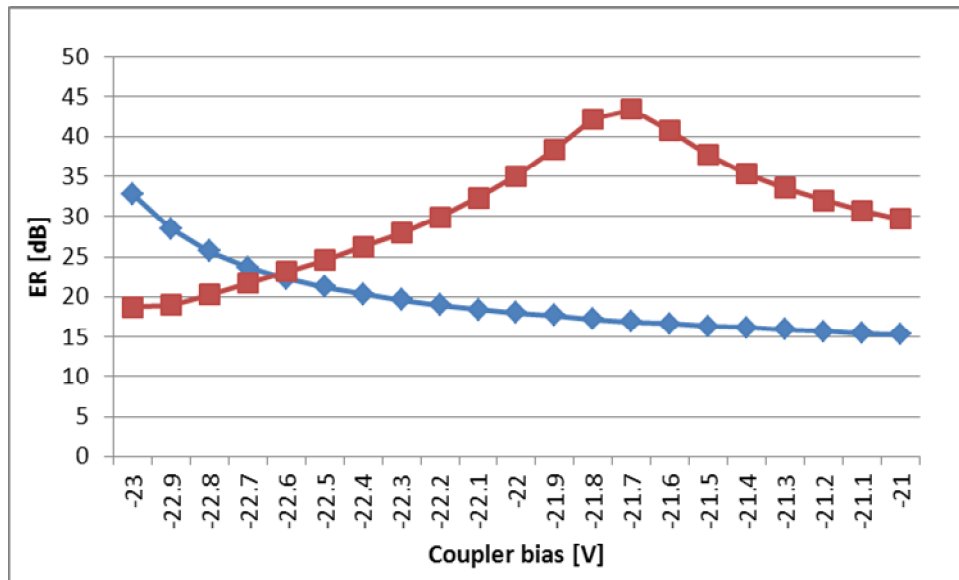


Figure 3.22. Coupler bias vs Output Er for coupler3 of MZ3 at temp. 27

Now to check the effect of temperature on demux some series of experiments have also been performed on different temperature i-e at 22 °C and then collect the results. The procedure applied is the same as above but the results are different as shown in below graphs.

Temperature 22 °C

From the below graph, the coupler bias voltage for coupler1 is -19.9 V and the extinction ratio is almost 26 dB. This shows that due to the change in the temperature the voltage shifted as compared to the previous value of the same coupler.

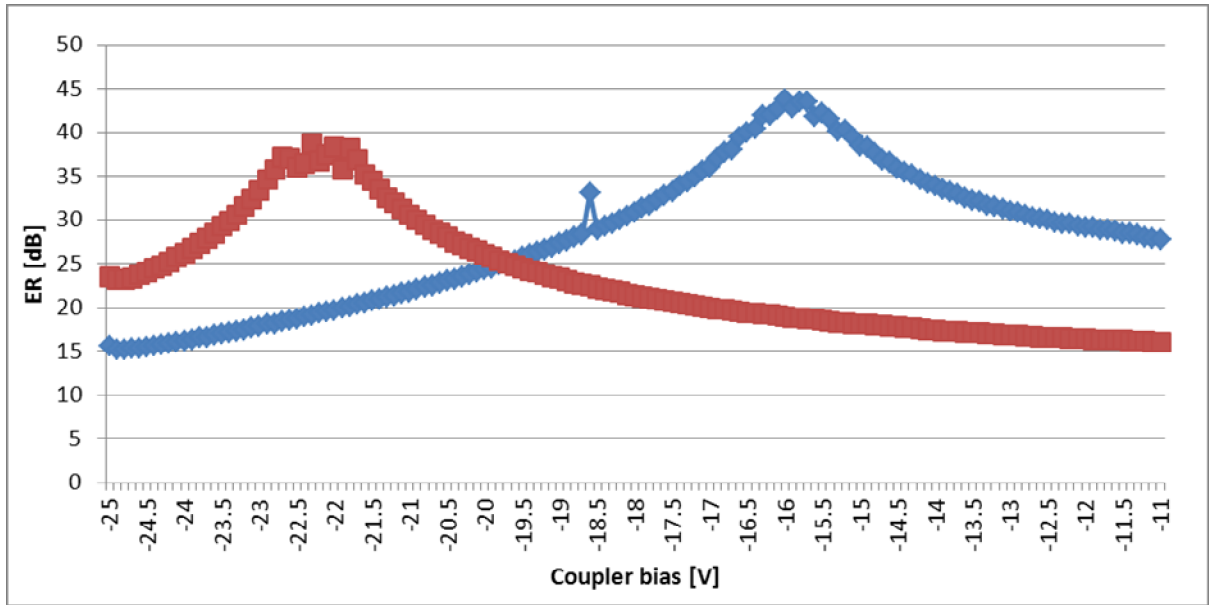


Figure 3.23. Coupler bias vs Output Er for coupler1 of MZ1 at temp. 22

The coupler bias voltage for coupler2 is -25.9 V and the extinction ratio is almost 22.7 dB as shown in the below graph. This also shows the shift in the voltage.

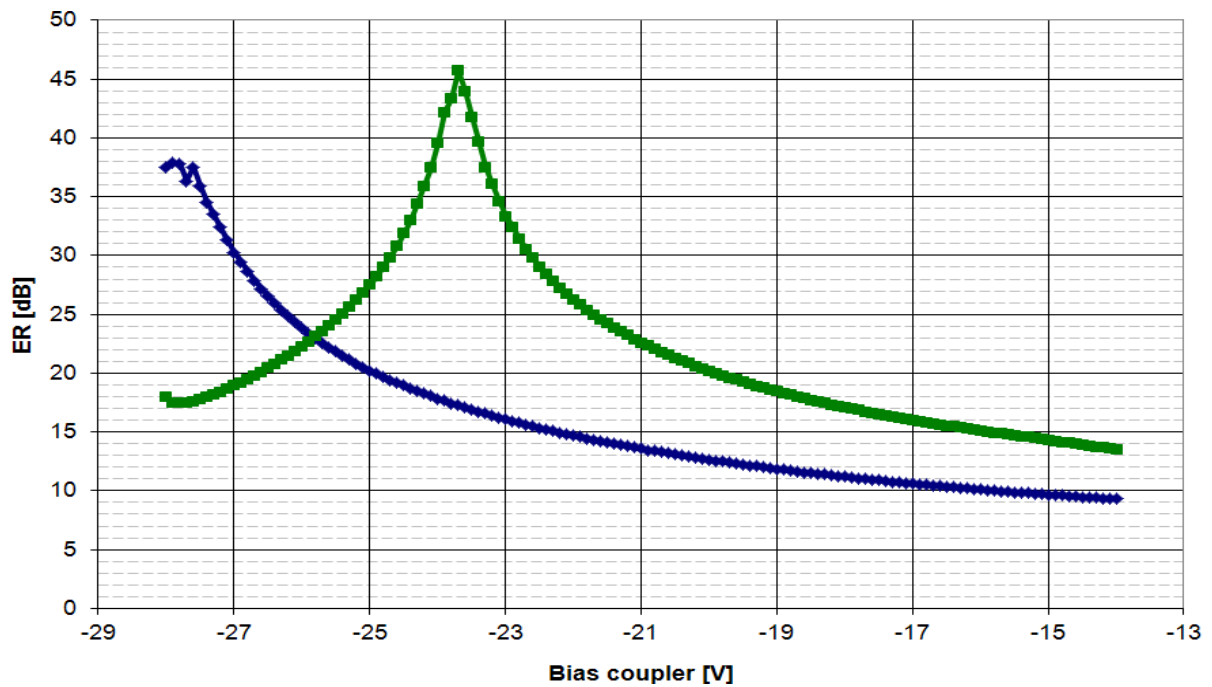


Figure 3.24. Coupler bias vs Output Er for coupler2 of MZ2 at temp. 22

The coupler bias voltage for coupler3 is -21.2 V and the extinction ratio is almost 23.6 dB as shown in the below graph. If this voltage value is compared with the previous

value taken at different temperature of the same coupler, shift can also be observed due to the temperature.

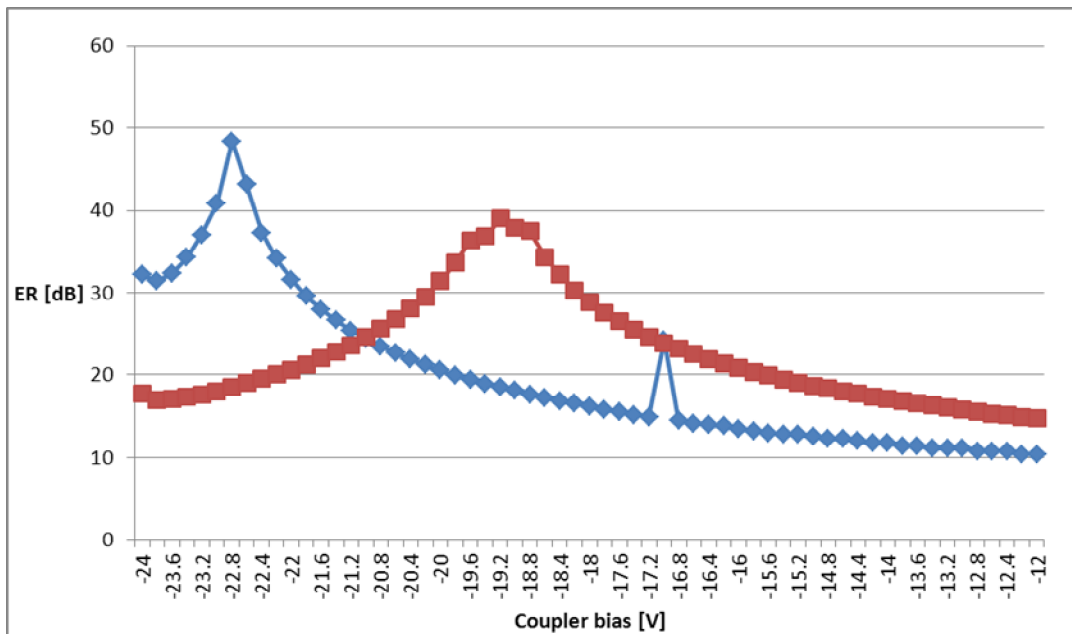


Figure 3.25. Coupler bias vs Output Er for coupler3 of MZ3 at temp. 27

3.2.5. Critical Observations

In order to check the stability of demux over temperature, different experiments has been performed on the same coupler and MZ at the same temperature. The graph of only MZ2 at 27 °C temperature are shown below, consider also the graph of MZ2 giving -22V and ER 23dB at 27 °C temperature showed above. For each new experiment the values for coupler and MZ bias has been changed but temperature is fixed. It is observed that there is a drift in 50/50 coupling voltage, which means un-stability.

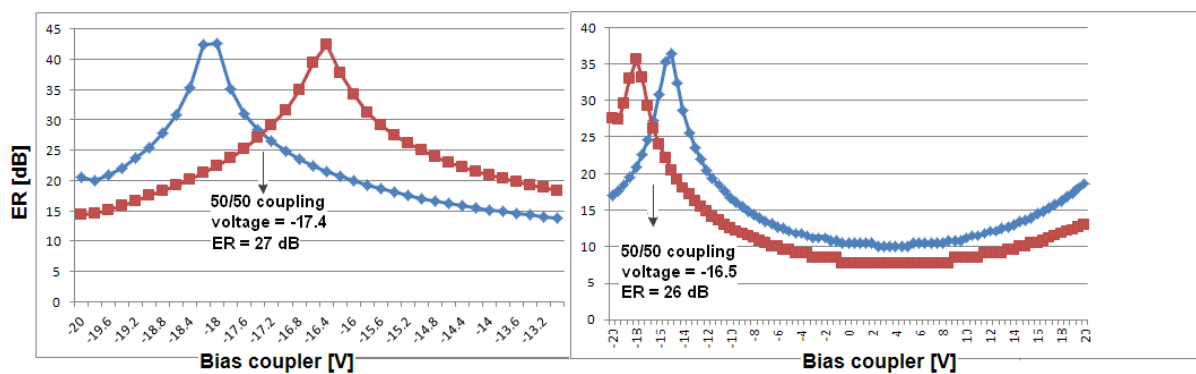


Figure 3.26. Drift in coupler bias voltage at same temperature

The reason can be that the temperature of the crystal doesn't remain stable. We have used the temperature stabilizer but it is not able to stabilize the temperature of the crystal to large extent. In order to reach the high extinction ratio requirement i-e more than 30dB, we need stabilize coupling and MZ bias. This temperature instability will also affect the quadrature bias voltage of MZ and hence the extinction ratio. At-last it is worth mentioning here that in order to stabilize the bias we can't even use the Bias Control Loop circuit (BCL) because it works if the modulation is zero mean. In our case the driving (clock) signal is synchronous with the optical signal, so the mean output power will be different from different outputs.

The next step in the characterization is to find the $V\pi$ and then the bias voltages for each MZ involve in the demux. To calculate this value we need the driving signal and for that we need frequency dividers and low noise amplifiers which should be precisely tuneable to meet the phase (90° shift at 200MHz) and gain requirement. To reach an ENOB of 10 bits the time/amplitude jitter of the demux must be less than 30dB.

$$\Delta amp = \cos^2(\Delta V / V\pi)$$

To have $\Delta amp < 0.1\%$ the voltage error must be lower than 2%. The amplitude error is also due to the time jitter, so it's better stay below 1%. Moreover, to reach 30dB ER, the error on the $V\pi$ measure must be less than 2%.

4. Conclusion

In order to summarize the whole work, the results that have been taken during a series of experiments allow us to check the performance of the demux and to find the issues regarding the control of demux which will lead to the bases for the next work in photonic assisted radar research. As far as impedance matching is concerned the required results have been met. Regarding the control of the demux, it can be finally concluded that we can attain what we are looking for if it is controlled well. By following the coupler bias vs E_r curves, in the last chapter, it can be concluded that demux can give high E_r if it is controlled well. There are some issues, regarding the instability, in the control of demux which should be addressed and can be covered if tuned well. Experiments on demux are still going on in the Lab; below I will mention what is the current status of the experiment.

4.1. Current Status of Experiments

The experimental setup on which current activities has been performed is shown in the Figure 4.1 below. In this preliminary activity all the control parameters have been manually adjusted in order to obtain the best performance and compensate some unexpected

problems, like the phase ambiguity of the clock dividers and stability. In our scheme both the 200MHz and the 100MHz driving signals are obtained by a division of the MLL' clock at 400MHz, so they apparently can't be locked in phase.

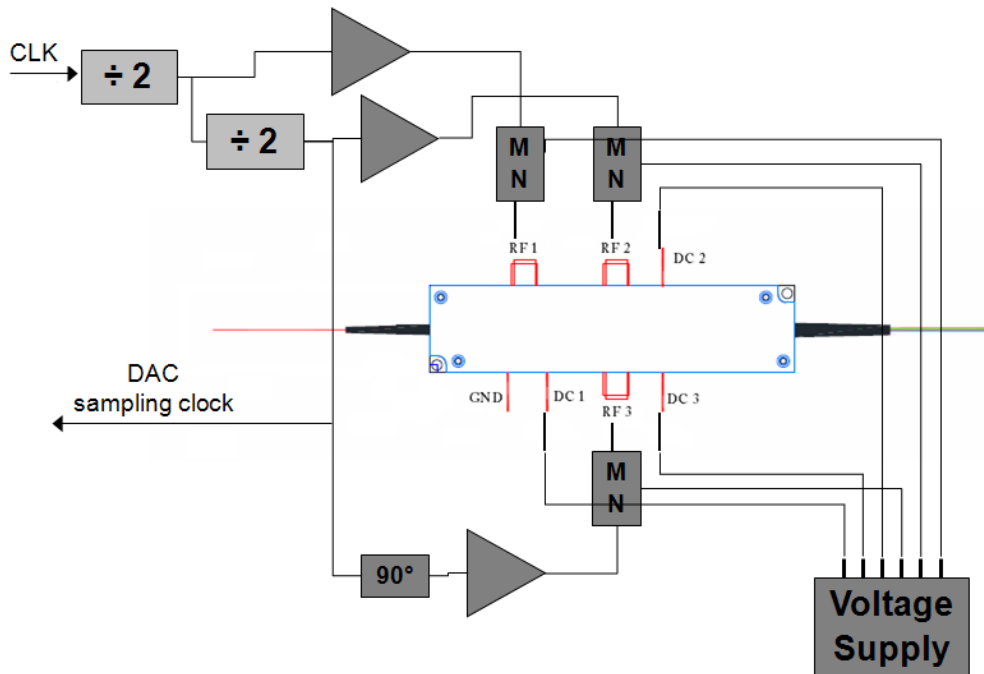


Figure 4.1. Experimental setup

Now the experiments have been performed by considering the deriving signals as well and for that low noise amplifiers (LNA) have been designed. Rest of the text will be on designing of LNAs and latest experimental results.

4.1.1. Driving Signal amplification and tuning

In order to provide the driving signals to the switching matrix, two different types of electrical amplifiers have been designed and realized: one single input double output 100 MHz low noise amplifier and one 200 MHz single input single output amplifier. Peculiar characteristics of the designed amplifiers are the very precise tunability of the operative gain and of the phase of the output signals. In Figure 4.2 and Figure 4.3 the electrical schemes of the two amplifiers are shown.

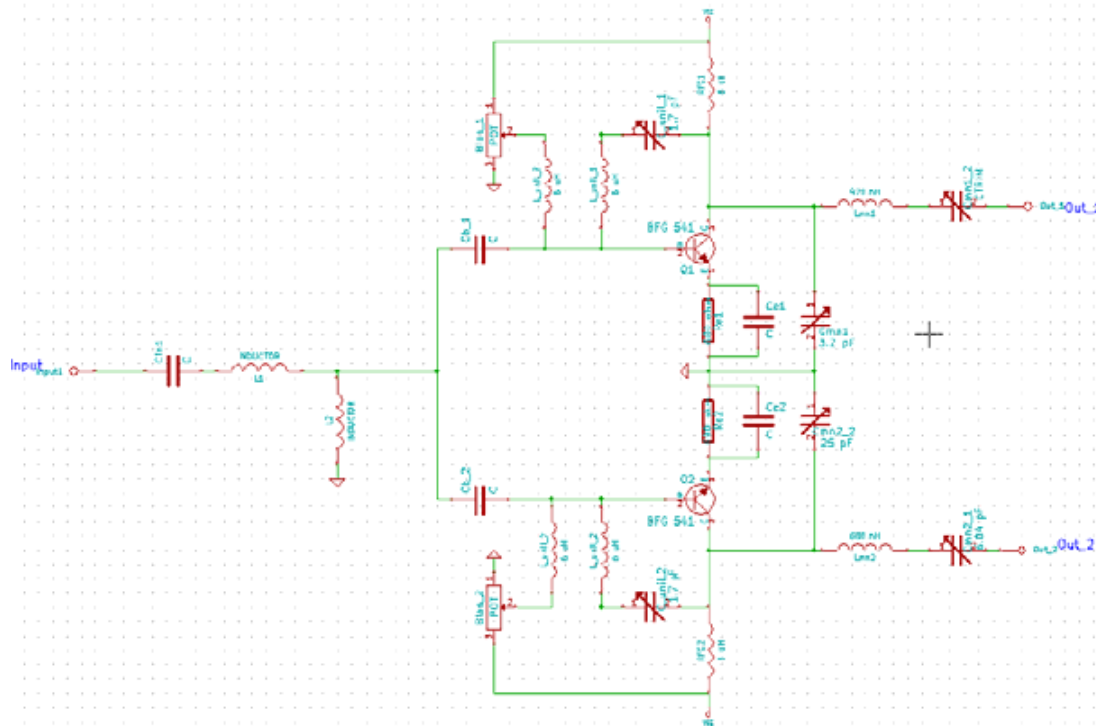


Figure 4.2. Single Input double output low noise 100 MHz amplifier

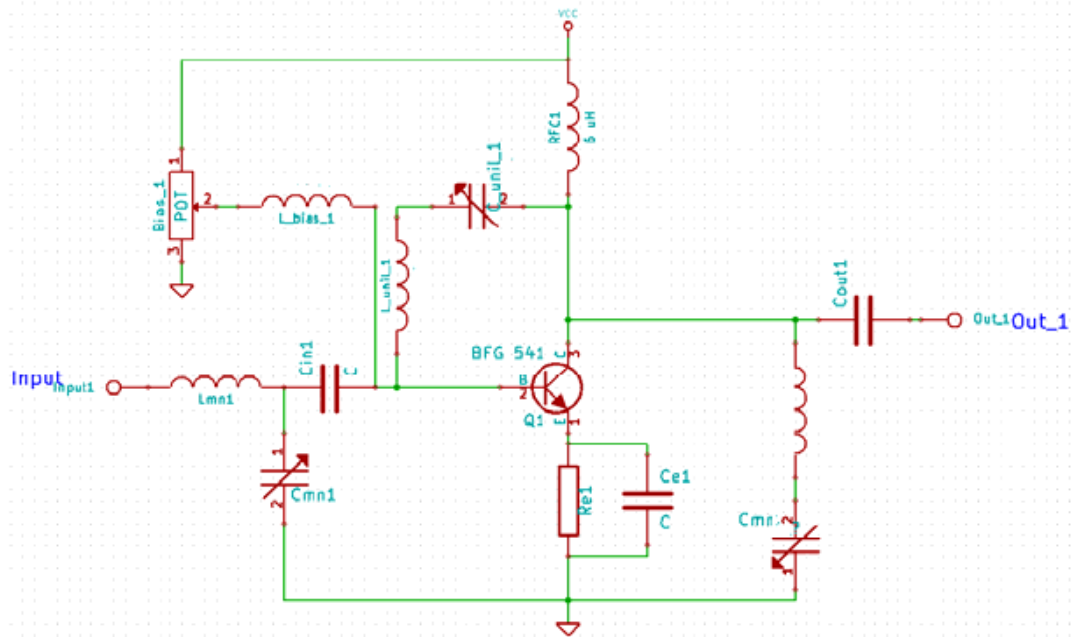


Figure 4.3. Single input single output low noise 200 MHz amplifier

The design specifications of the two amplifiers are listed in the table below:

	100 MHz Amplifier	200 MHz Amplifier
Nominal Gain	23.5 dB	14.2 dB
Noise Figure	< 7 dB	< 7 dB
Output Amplitude tunability	± 2 dB	± 2 dB
Output Phase tunability	$\pm 10^\circ$	$\pm 10^\circ$

Both amplifiers are based on a low noise and high gain Bipolar Junction Transistor (BJT). Due to the operational constraints of the optical de-multiplexer a precise tuning of the amplifiers gain and of the output phase is needed. The gain, can be finely tuned, thanks to the small tuning range needs, by slightly changing the working point of the BJT, without affecting significantly the noise figure NF of the device, that is, in all the tuning range, lower than the design specifications. For what concern the phase tuning, this can be changed by acting on the output matching network. The 100 MHz device provide also a 90° phase shift between the two outputs, in order to match the shift requirement for the driving signals of the second stage of the switching matrix.

4.1.2. Experiment Results

The current experimental results reported has led to an effective number of bit (ENOB) equal to 5.27, while the targeted ENOB was >8 . The obtained number is largely limited by the reduced dynamic range of the sampled pulses at the ADC, which only cover 11mV out of 200mV (minimum input range for the ADC). The second cause for reduced ENOB is the noise generated in the optical and electrical amplification stages.

On the other hand, the FFT spectrum in below Figure 4.4 does not show the spurious components that characterize the sampling processes affected by crosstalk. This suggest the correct behaviour of the switch matrix, even if it is used here as a demultiplexer.

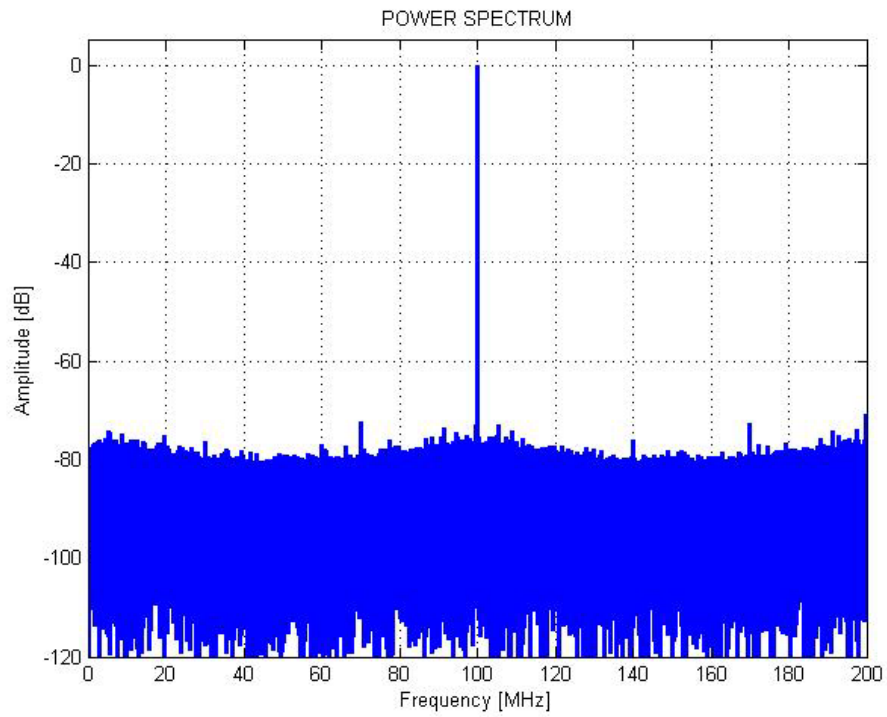


Figure 4.4. Spectrum of the reconstructed signal.

The next activity will be to fully exploit the switching functionality of the matrix, setting all the bias voltages and optimizing all the driving signals.

5. References

1. R. Rzemien, “Coherent Radar: Guest Editor’s Introduction,” John Hopkins APL Technical Digest, 1997.
2. R. H. Walden, “Analog-to-Digital Converter Survey and Analysis”, IEEE J. Sel. Areas Commun., vol 17, no. 4, pp. 539-550
3. Le Nguyen Binh, “Photonic Signal Processing, Techniques and Application”.
4. <http://www.ntt.com/worldwide/resource-center/article/data/global-watch02.html>
5. S. J. Ben Yoo, Fellow, IEEE , “Energy Efficiency in the Future Internet: The Role of Optical Packet Switching and Optical-Label Switching”, IEEE Journal of Selected Topics In Quantum Electronics, Vol. 17, No. 2, March/April 2011
6. Shacham, A.; Small, B.A.; Liboiron-Ladouceur & O.; Bergman, K., (2005). A fully implemented 12x12 data vortex optical packet switching interconnection network. IEEE Journal of Lightwave Technology, Vol. 23, No. 10, (Oct. 2005) pp. 3066-3075, 0733-8724.
7. K. Wilner and A.P. van der Heuvel, “Fiber-optic delay lines for microwave signal processing”, Proc. IEEE, 64(5), 805–807, 1976.
8. M. Scaffardi, P Ghelfi, C. Porzi, G. Meloni, G. Berrettini, A. Malacarne, F. Fresi, E. Lazzeri, J. Wang, X. Wu, I. Fazal, A. Willner, L. Potì, A. Bogoni, “ Photonic Digital Processing for Enabling Next Generation Optical Networks”, IEEE, 2009.
9. C. Porzi, et al, “All-optical NAND/NOR Logic Gates with Passive Nonlinear Etalon Exploiting Absorption Saturation in Semiconductor MQWs”, IEEE 2007
10. R. H. Walden, “Analog-to-Digital Converter Survey and Analysis”, IEEE J. Sel. Areas Commun., vol 17, no. 4, pp. 539-550

11. M. P. Fok, K. L. Lee, C. Shu, "4 x 2.5 GHz Repetitive Photonic Sampler for High-Speed Analog-to-Digital Signal Conversion", IEEE Photon. Technol. Lett., vol. 16, no. 3, pp. 876-878 March 2004.
12. <http://www.radartutorial.eu>.
13. Merrill I. Skolnik, "Introduction to Radar Systems", 2nd Edition.
14. Mark A. Richards, James A. Scheer, William A. Holm, "Principals of Modern Radar: Basic Principals "
15. Michael E. Yeomans, "Chapter 6 of Radar Handbook by Merrill Skolnik".
16. Paolo Ghelfi, et al. "Ultra-stable Radar signal from a Photonics-Assisted transceiver based on single Mode-Locking Laser", OSA/OFC/NFOEC 2011.
17. Paolo Ghelfi, et al. "Photonic generation of Phase-Modulated RF signals for pulse compression techniques in Coherent Radars", IEEE 2011.
18. Paul W. Juodawlkis, et al, "Optically Sampled Analog-to-Digital Converters", IEEE Transactions on Microwave theory and Tchniques, VOL. 49, NO. 10, OCTOBER 2001.
19. George C. Valley," Photonic analog-to-digital converters", 2007 Optical Society of America.